Molecular Therapy
Methods & Clinical Development
Original Article

Efficient and safe correction of hemophilia A by lentiviral vector-transduced BOECs in an implantable device

Cristina Olgasi,[1,12] Chiara Borsotti,[1,12] Simone Merlin,[1,12] Thorsten Bergmann,[2] Patrick Bittorf,[2] Adeolu Badi Adewoye,[3] Nicholas Wragg,[4] Kelcey Patterson,[5] Andrea Calabria,[6] Fabrizio Benedicenti,[6] Alessia Cucci,[1] Alessandra Borchiellini,[7] Berardino Pollio,[8] Eugenio Montini,[6] Delfina M. Mazzuca,[5] Martin Zierau,[9] Alexandra Stolzing,[10,11] Philip.M. Toleikis,[5] Joris Braspenning,[2] and Antonia Follenzi[1]

[1]Department of Health Sciences, University of Piemonte Orientale, 28100 Novara, Italy; [2]Department of Tissue Engineering and Regenerative Medicine, University Hospital Würzburg, 97082 Würzburg, Germany; [3]Institute of Inflammation and Ageing, College of Medical and Dental Sciences, University of Birmingham, B15 2TT Birmingham, UK; [4]Guy Hilton Research Centre, School of Pharmacy and Bioengineering, Keele University, Staffordshire, ST47QB Stoke-on-Trent, UK; [5]Sernova Corp., London, ON N6G4X8, Canada; [6]TIGET-HSR, 20132 Milan, Italy; [7]Haematology Unit Regional Center for Hemorrhagic and Thrombotic Diseases, City of Health and Science University Hospital of Molinette, 10126 Turin, Italy; [8]Immune-Haematology and Transfusion Medicine, Regina Margherita Children Hospital, City of Health and Science University Hospital of Molinette, 10126 Turin, Italy; [9]IMS Integrierte Management Systeme e. K., 64646 Heppenheim, Germany; [10]Centre for Biological Engineering, School of Mechanical, Electrical and Manufacturing Engineering, Loughborough University, LE113TU Loughborough, UK; [11]SENS Research Foundation, Mountain View, CA 94041, USA

Hemophilia A (HA) is a rare bleeding disorder caused by deficiency/dysfunction of the FVIII protein. As current therapies based on frequent FVIII infusions are not a definitive cure, long-term expression of FVIII in endothelial cells through lentiviral vector (LV)-mediated gene transfer holds the promise of a one-time treatment. Thus, here we sought to determine whether LV-corrected blood outgrowth endothelial cells (BOECs) implanted through a prevascularized medical device (Cell Pouch) would rescue the bleeding phenotype of HA mice. To this end, BOECs from HA patients and healthy donors were isolated, expanded, and transduced with an LV carrying FVIII driven by an endothelial-specific promoter employing GMP-like procedures. FVIII-corrected HA BOECs were either directly transplanted into the peritoneal cavity or injected into a Cell Pouch implanted subcutaneously in NSG-HA mice. In both cases, FVIII secretion was sufficient to improve the mouse bleeding phenotype. Indeed, FVIII-corrected HA BOECs reached a relatively short-term clinically relevant engraftment being detected up to 16 weeks after transplantation, and their genomic integration profile did not show enrichment for oncogenes, confirming the process safety. Overall, this is the first preclinical study showing the safety and feasibility of transplantation of GMP-like produced LV-corrected BOECs within an implantable device for the long-term treatment of HA.

INTRODUCTION

Hemophilia A (HA) is an X-linked disorder caused by mutations in the *F8* gene.[1,2] These mutations result in deficiency or reduced activity of the coagulation factor VIII (FVIII), leading to a life-long bleeding tendency, whose clinical severity is proportional to FVIII reduction.[1] Although the current standard of care is to intravenously infuse HA patients with clotting factor concentrates, the short half-life of FVIII requires frequent and multiple infusions, with a negative impact on the patient's quality of life (QoL). A new generation of standard rFVIII was obtained by refinements of the recombinant protein through the optimization of relevant post-translational modifications, such as glycosylation, that improve the stability of the mature FVIII protein,[3] or the introduction of a covalent link between the FVIII heavy and light chains, preserving FVIII from premature degradation and conferring a higher binding affinity to von Willebrand factor (vWF) with a reduction of the needed injection dose.[4–6]

Other new bioengineered molecules were developed with higher extended plasma half-life[7] and improved pharmacokinetics by the fusion of rFVIII with the Fc portion of immunoglobulin[8] or by conjugation with polyethylene glycol (PEGylation).[9]

However, several issues are still to be solved as the recurrent intravenous (i.v.) route of administration and the inhibitor development, common in 20%–40% of patients with the severe form,[10] worsen the clinical outcome, making the treatment ineffective.[11,12] Therefore, a new clinical approach emerged more recently, i.e., emicizumab, to overcome the difficulties of i.v. delivery and to improve and prolong the effectiveness of the therapy in all patients, regardless of the presence or absence of the inhibitor.[13,14]

Received 30 June 2021; accepted 29 October 2021;
https://doi.org/10.1016/j.omtm.2021.10.015.

[12]These authors contributed equally

Correspondence: Antonia Follenzi, MD, PhD, Department of Health Sciences, School of Medicine, Università del Piemonte Orientale "A. Avogadro," 28100 Novara, Italy.
E-mail: antonia.follenzi@med.uniupo.it

However, bleeding events can still occur after trauma, requiring the use of additional hemostatic agents according to the patients' inhibitor status.[15,16]

This has led researchers to explore innovative cell and gene therapy strategies that may ensure continuous endogenous FVIII expression with only a one-time treatment. Another good reason for choosing gene therapy over traditional approaches is that HA is a monogenic disease, i.e., entirely ascribable to the lack of one protein, FVIII, and that a small increase in FVIII plasma levels is enough to ameliorate the bleeding phenotype of HA patients.

Given the growing number of cell and gene therapy approaches being developed, it is becoming increasingly important to identify the most suitable cell target. Even though *F8* mRNA is expressed in different human and mouse organs, such as liver, spleen, lymph nodes, kidney,[17–20] and in hematopoietic cells,[21,22] transplantation studies in hemophilic animal models have shown FVIII expression to be mainly localized in liver sinusoidal endothelial cells (LSECs),[23–25] making these cells attractive targets for HA gene therapy. This is also supported by the fact that endothelial cells (ECs) secrete FVIII and can act as tolerogenic cells.[24,26]

Over the years, several gene therapy approaches for HA have been attempted using adeno-associated virus (AAV) vectors to induce FVIII expression in the desired cell type. Despite the encouraging preliminary results obtained in few ongoing clinical trials testing the efficacy of AAV-mediated hepatocyte-targeted FVIII expression in HA patients,[27–29] some medical issues still need to be addressed, such as the use of these vectors in patients with pre-existing immunity to AAV or with FVIII inhibitors. As AAV vectors do not actively integrate into the host cell genome, they are lost upon cell division during liver growth or in case of liver disease, thus potentially limiting their use in pediatric patients and questioning their life-long maintenance. Therefore, lentiviral vectors (LVs) could represent a viable approach able to overcome some AAV limitations. Moreover, several studies have demonstrated, by the use of endothelial-specific promoters, specific expression of human FVIII in LSECs.[23–25,30] Recently, we have shown that induced pluripotent stem cells (iPSCs) derived from $CD34^+$ HA cells can be differentiated into ECs and genetically corrected by LV to express the FVIII transgene, deleted of the B domain (BDD), driven by the endothelial-specific vascular endothelial cadherin (VEC) promoter. After transplanting these cells into the liver of monocrotaline-conditioned NOD-*scid* $IL2Rg^{null}$ HA (NSG-HA) mice, we were able to correct the bleeding phenotype of these mice and maintain a stable FVIII activity over time.[31] Moreover, BDD-FVIII-transduced ECs encapsulated in microcarrier beads have been shown to survive for a prolonged time in the peritoneal cavity of NSG-HA mice secreting therapeutic levels of FVIII.[31]

Several studies have focused on defining different cell sources and matrices to transplant FVIII-expressing ECs.[32–34] A readily available EC source is represented by patient-derived blood outgrowth endothelial cells (BOECs).[35] BOECs are isolated from adult peripheral blood[36] and can be fully differentiated into mature ECs. They promote neovascularization *in vivo* when transplanted into immunodeficient mice[37] or when cultured on three-dimensional biodegradable vascular scaffolds.[38–40] In addition, they can be considered a valuable source of cells to understand EC biology and model disease, and can be used in regenerative medicine due to their ability to promote neovascularization, thus representing an optimal candidate for HA cell and gene therapy. Indeed, BOECs transplanted in NSG-HA mice after gene modification for FVIII expression were able to partially rescue the hemorrhagic phenotype of these mice.[35,41] Moreover, autologous transplantation of FVIII-expressing BOEC cell sheet allowed long-term phenotypic correction and survival of transplanted cells.[34] Noteworthy, BOECs can promote neovascularization *in vivo* in combination with synthetic or natural materials.[37]

A combination of LV-corrected BOECs with a medical device is classified by the European Union as a combined gene therapy medicinal product (GTMP).[42] The mandatory non-clinical study scheme before the first administration of a cell-based GTMP to human subjects includes the comprehensive characterization of the transduced cells and the evaluation of the medical device contribution.[43] Moreover, the proof-of-concept pharmacodynamics along with the molecular mechanism of action must be identified in preclinical models *in vivo* and/or *in vitro*. These studies are deemed essential to determine the GMP cell dose to be used in clinical trials.[44]

Here, we show extensive characterization of LV-transduced BOECs isolated from healthy donors or HA patients for FVIII production *in vivo*. These cells were transplanted in a small scalable, implantable, and prevascularized medical device, namely Cell Pouch (Sernova), previously developed for diabetes treatment.[45]

Our findings, showing that Cell Pouch-transplanted LV-corrected HA BOECs are capable of correcting the bleeding phenotype of HA mice, open new avenues for the treatment of HA in humans.

RESULTS

Characterization of BOECs isolated from HA patients or healthy subjects and LV-mediated FVIII gene transfer

Upon isolation and expansion in culture medium, both BOECs from healthy donors and HA patients showed the classical endothelial cobblestone-like morphology (Figure 1A). Of note, despite being all isolated from severe HA patients, HA BOECs gave rise to many colonies (Figure S1A) and there was not a significant difference in the number of isolated colonies between healthy donors and HA patients (Figure S1B). For transgene expression, isolated cells were transduced with a LV carrying the BDD form of FVIII driven by the vascular endothelial cadherin promoter (LV-VEC.hBDD-FVIII) or with an LV carrying the green fluorescent protein under the control of the same promoter (LV-VEC.GFP), both at an multiplicity of infection (MOI) of 20. FACS analysis showed 98% ± 1% GFP^+ cells after transduction (Figure S1C), indicating excellent transduction efficiency. The number of integrated LV copies/cell was ~6 and ~3 for

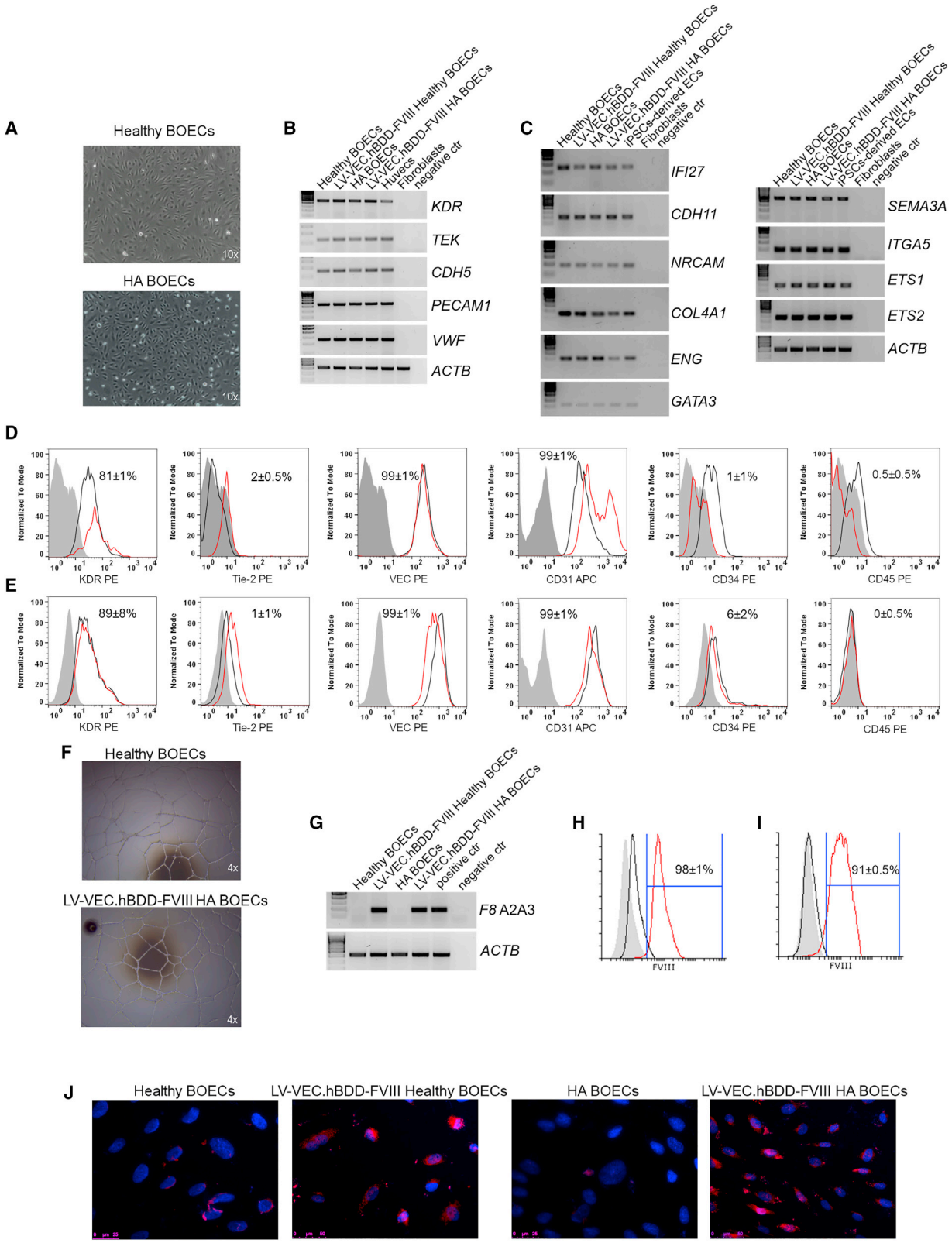

(legend on next page)

LV-VEC.GFP- and LV-VEC.hBDD-FVIII-transduced cells, respectively (Figure S2A). Thus, this protocol ensures a very high transduction efficiency while maintaining a safe number of integrated LV copies/cell.[46,47]

We next assessed the endothelial phenotype and functionality of transduced versus non-transduced healthy or HA BOECs. As shown in Figure 1B, all cells expressed classical endothelial markers (e.g., *PECAM1*, *KDR*, *TEK*, *CDH5*, and V*WF*) as well as other genes specific to blood endothelial cells (BECs)[48,49] (Figure 1C). The endothelial phenotype of healthy and HA BOECs was further verified at the protein level (Figures 1D and 1E, respectively), while the hematopoietic phenotype was ruled out upon CD34 and CD45 staining, which resulted negative (Figures 1D and 1E).

The endothelial functionality of the transduced cells was confirmed by their ability to form tubule networks upon Matrigel cell culture (Figure 1F). *F8* mRNA expression was measured in transduced BOECs by RT-PCR (Figure 1G), while FVIII protein expression levels were detected by flow cytometry (see Figures 1H and IJ for healthy and HA BOECs, respectively) and immunofluorescence (IF) (Figure 1J). Interestingly in healthy BOECs we detected low levels of FVIII (Figures 1H and 1J). This is in accordance with previous works where FVIII in healthy BOECs was barely observed.[41,50,51] When cell supernatants were subjected to activated partial thromboplastin time (aPTT) assay, we noticed a consistent shortening in LV-VEC.hBDD-FVIII-transduced BOECs (69 ± 3.5 s for transduced healthy BOECs, 66 ± 4 s for transduced HA BOECs) compared with non-transduced cells (80 ± 2.8 s for healthy BOECs, 84 ± 2.8 s for HA BOECs) (Figure S2B), in good agreement with the amount of secreted FVIII (35.9 ± 2.3 ng/mL for LV-VEC.hBDD-FVIII healthy BOECs, 4.5 ± 1.3 ng/mL for non-transduced healthy BOECs; 54 ± 7.5 ng/mL for LV-VEC.hBDD-FVIII HA BOECs, 0.15 ± 2.5 ng/mL for non-transduced HA BOECs) (Figure S2C).

To further evaluate the safety of LV transduction, healthy BOECs were transduced with different MOIs (MOI = 10, 20, 50, or 100), and HIV-1 p24 expression on cell supernatant was assessed. As shown in Figure S2C, all LV-transduced BOEC supernatants were negative for HIV-1 p24 at any of the MOIs tested 10 days after transduction, suggesting the reliability of our protocol. HIV-1 p24 on supernatant of HA BOECs transduced with an MOI of 20 showed comparable results (Figure S2D).

Secretion of the FVIII gene product by LV-transduced HA or healthy BOECs in NSG-HA mice

Since healthy and HA BOECs were both able to secrete FVIII *in vitro*, we evaluated their ability to survive and secrete FVIII in NSG-HA mice after intraperitoneal injection in association with Cytodex 3 microcarrier beads. Following injection, FVIII-transduced GFP$^+$ healthy BOECs were able to partially restore FVIII activity, which reached a peak of approximately 10% at 4 weeks post injection (pi) and persisted above 5% for up to 10 weeks pi (Figure 2A). As expected, LV-VEC.GFP BOEC controls showed only basal FVIII secretion, which only lasted for 4 weeks. Importantly, mice receiving FVIII-transduced HA BOECs revealed sustained therapeutic FVIII activity (up to 10%) for up to 13 weeks pi, which persisted at a level <5% throughout the following 18 weeks (Figure 2A). Blood loss assays, run between 7 and 10 weeks pi of FVIII-transduced GFP$^+$ HA BOECs, demonstrated partial restoration of hemostasis (Figure 2B) accompanied by detectable amounts of plasmatic FVIII antigen (12.4 ± 3.9 ng/mL) (Figure 2C). At week 13 pi, three mice in each experimental group were killed, and beads were recovered from the abdominal cavity. IF staining was performed on the recovered beads using an anti-GFP antibody that would detect the transplanted cells that were previously transduced with both LV-VEC.GFP and LV-VEC.FVIII. Therefore, the presence of GFP$^+$ cells confirm that they are still associated with the beads and that they maintained an endothelial phenotype, as shown by the co-staining with CD31 (Figure 2D).

Large-scale expansion of FVIII-transduced cells

With the aim to translate this approach into the clinic, we developed a protocol that would allow us to obtain a large amount of transduced HA BOECs for our *in vivo* experiments. LV-VEC.hBDD-FVIII-transduced HA BOECs from four patients were large-scale expanded to reach 10^8 cells, frozen, and sent to the partners in accordance with GMP-like procedures. Upon arrival, cells were re-cultured by simulating a centralized cell production process with long-term cryopreservation. After large-scale expansion and cryopreservation, upon thawing and reseeding, all cells showed normal cobblestone-like morphology (Figure 3A). Even though they were slightly enlarged, no significant changes in their doubling time, cell density, and length of time required for expansion were noticed (Figure 3B). In addition to maintaining expression of the classical endothelial markers (CD31, KDR, Tie-2, and VEC), expanded BOECs became CD34$^+$, a transmembrane phosphoglycoprotein involved in cell adhesion,[52] while they retained the classical CD45$^-$ phenotype (Figure 3C).

Figure 1. Healthy and HA BOEC isolation, LV transduction, and *in vitro* FVIII detection

(A) Light microscope pictures of cultured healthy and HA BOECs at passage 3. (B) Representative RT-PCR analysis for the expression of endothelial markers. HUVECs and fibroblasts were used as positive and negative control, respectively. (C) RT-PCR for endothelial markers specific for blood endothelial cells (BECs). iPSC-derived ECs and fibroblasts were used as positive and negative control, respectively. (D) Representative histograms of healthy non-transduced (black line) and LV-VEC.hBDD-FVIII-transduced healthy BOECs (red line), showing endothelial marker expression and absence of hematopoietic markers. The filled-up histograms represent unstained BOECs. (E) Representative histograms of HA non-transduced (black line) and LV-VEC.hBDD-FVIII-transduced HA BOECs (red line) showing endothelial marker expression and absence of hematopoietic markers. The filled-up histograms represent unstained BOECs. (F) Matrigel assay confirming tubule formation of transduced BOECs. (G) RT-PCR, using primers specific for the exogenous *F8* in non-transduced and LV-VEC.hBDD-FVIII BOECs. Unrelated transduced cells and fibroblast were used as positive and negative control, respectively. (H) FVIII intracytoplasmic staining on non-transduced (black line) or transduced healthy BOECs (red line). The filled-up histogram represents unstained BOECs. (I) FVIII intracytoplasmic staining on non-transduced (black line) or transduced HA BOECs (red line). The filled-up histogram represents unstained BOECs. (J) FVIII detection by immunofluorescence: blue, DAPI; red, anti-FVIII. Data are expressed as mean ± SD and are representative of four independent experiments.

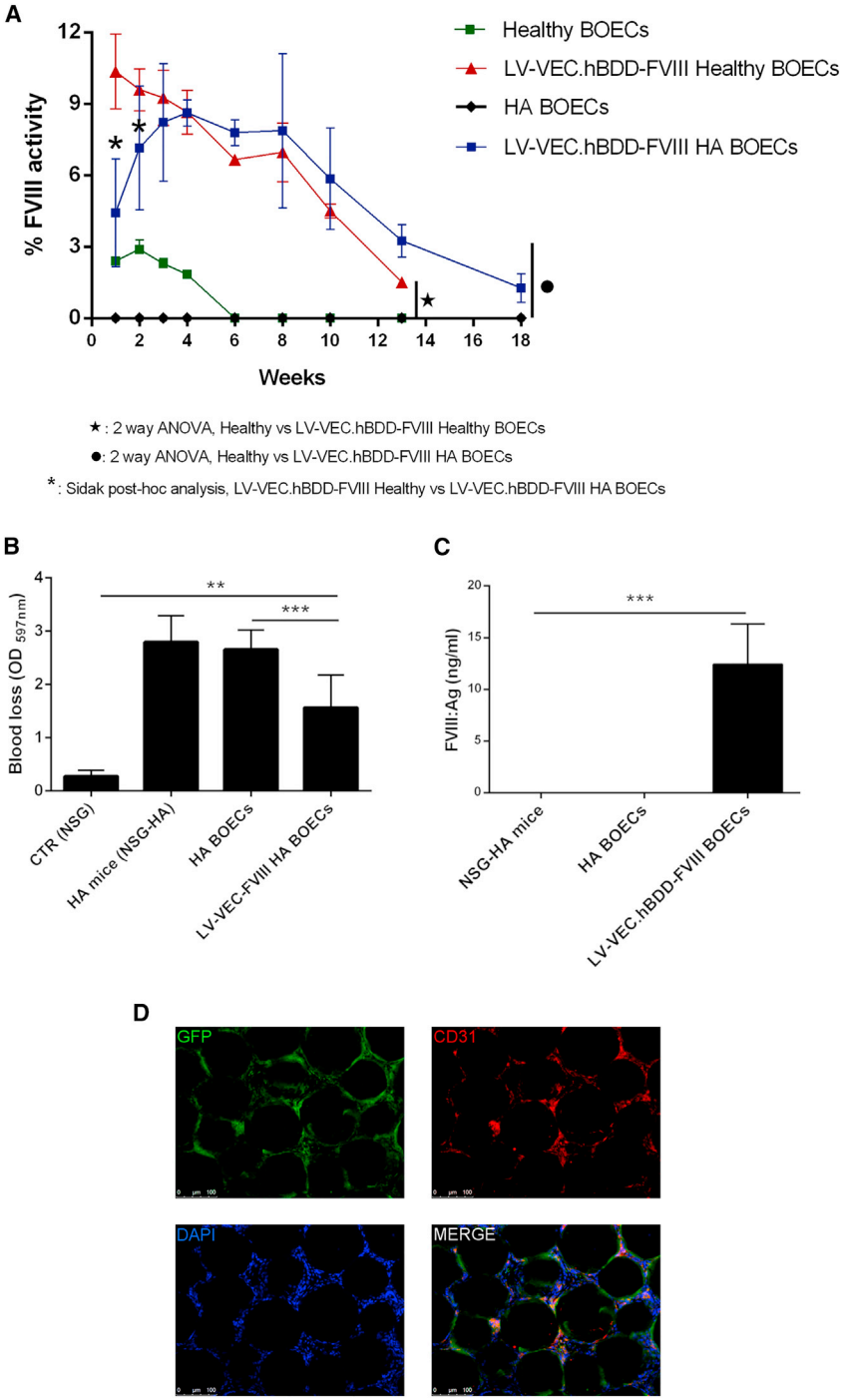

Figure 2. Intraperitoneal implantation of BOECs with Cytodex microcarrier beads

(A) Kinetics of the percentage of FVIII activity measured by aPTT assay in the plasma of transplanted NSG-HA mice. BOECs used were transduced only with LV-VEC.GFP or with both LV-VEC.hBDD-FVIII and LV-VEC.GFP. Data are expressed as mean ± SD and are representative of two independent experiments using BOECs from two healthy donors (n = 7 mice), and four independent experiments using HA BOECs from four patients (n = 23 mice). (B) Blood loss evaluation on NSG-HA mice between weeks 7 and 10 (n = 4) after cell transplantation. (C) FVIII concentration in plasma of mice transplanted with transduced or non-transduced BOECs at week 16. Data are expressed as mean ± SD (***$p < 0.0001$, **$p < 0.001$). (D) Representative immunofluorescence on beads showing cells co-expressing GFP and CD31.

Functionally, FVIII-transduced cells preserved their tubulogenesis activity (Figure 3D) and led to partial restoration of FVIII activity once transferred into NSG-HA mice (Figure 3E), similar to the kinetics of non-expanded BOECs. Thus, LV-VEC.hBDD-FVIII HA BOECs maintain their ability to secrete FVIII at therapeutic levels even after large-scale expansion.

Tissue matrix development and safety of LV-VEC.hBDD-FVIII-transduced BOECs within a Cell Pouch implanted in NSG-HA mice

The Cell Pouch is a medical implantation device specifically designed to enable the development of a vascularized tissue matrix environment that ensures long-term survival and function of transplanted therapeutic cells. Thus, we first evaluated the safety and survival of transduced HA BOECs within the Cell Pouch implanted in NSG-HA mice. For this purpose, 4-week implanted Cell Pouches were transplanted with one of three doses ($2\times$, $5\times$, or 10×10^6) of LV-VEC.hBDD-FVIII HA BOECs isolated from two separate HA donors. The Cell Pouches transplanted with BOECs were explanted at 4, 8, or 12 weeks, and a gross pathological assessment was performed. HA BOECs were safe across doses and time points with no visible tumors observed (n = 60 total; HA1 n = 37; HA2, n = 23) (data not shown).

Overall, the tissue matrix developed within the Cell Pouch internal chamber and transplant area was viable among all groups according to time, dose, and cell lot, with no apparent signs of inflammation, hemorrhage, fibrosis, or necrosis (Figure 4A; Table S1). The center of the transplanted chamber area showed mild to moderate collagen deposition without any difference due to donor lot, time, or dose. Within the area of pre-vascularization, there was a comparative increase in established collagen, indicating that the Cell Pouch promoted, over time, the development of a natural scaffold to provide strength and structure to the environment, irrespective of the transplant. Regarding tissue vascularization, there was moderate neovascularization of the central, transplanted tissue of the Cell Pouch that was present in

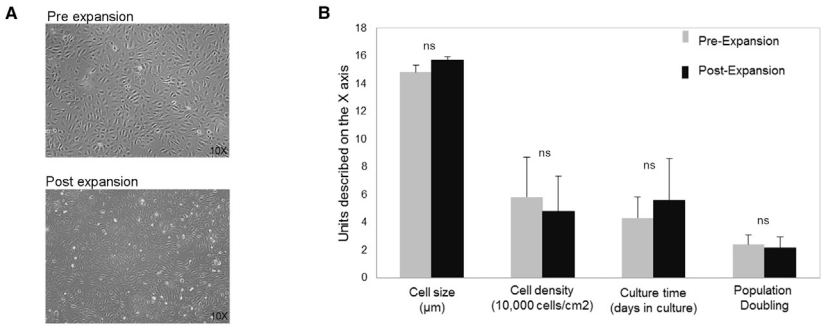

Figure 3. Large-scale expansion of HA patient-derived BOECs

(A) Light microscope pictures of transduced HA BOECs pre- and post-expansion. (B) Cell size, cell density, culture time, and population doubling level during pre- and post-large-scale expansion. (C) Endothelial marker expression pre- and post-large-scale expansion expressed as stained cells versus cells with secondary isotype controls. (D) Tubulogenic assay to assess the functionality of transduced HA BOECs after pre- and post-large-scale expansion. (E) Kinetics of the percentage of FVIII activity measured by aPTT assay in plasma of transplanted NSG-HA mice. Data are expressed as mean ± SD and are representative of two independent experiments (n = 7).

C

	Pre-expansion	Post-expansion
Surface markers	Expression (%)	Expression (%)
Tie2	3.9 ± 1.9	4.5 ± 1.0
KDR	20.9 ± 2.8	44.1 ± 3
CD45	2.9 ± 1.0	2.5 ± 2.4
CD34	3.5 ± 0.2	85.8 ± 0.9
CD31	99.1 ± 0.3	98.4 ± 1.0
VE-Cadherin	98.8 ± 0.4	96.1 ± 0.9

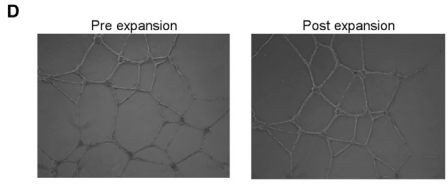

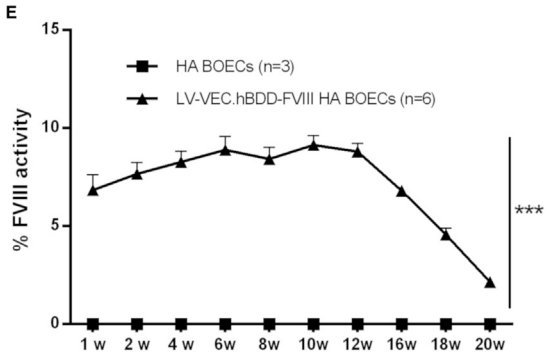

both donor lots, as well as the controls, along with evidence of established vessel growth, indicating that the tissue development within this area included new blood vessel formation (Figure 4B). Established vessels within the central, transplanted zone appeared to be more prominent and donor dependent at the latest time points (Figure 4A).

Transduced HA BOECs improve the bleeding phenotype and cell survival in mice after transplantation into the vascularized Cell Pouch

The therapeutic efficacy of LV-VEC.hBDD-FVIII HA BOECs transplanted into the Cell Pouch was evaluated by performing a tail bleeding assay on NSG-HA mice 4 months after cell transfer. Remarkably, we noticed a significantly improved presence of clotting as judged by a reduction in blood volume recovered in animals transplanted with 20×10^6 LV-VEC.hBDD-FVIII HA BOECs compared with non-transplanted mice (Figure 5A). Notably, this was not significantly different when compared with NSG mice, confirming that correction of the missing coagulation factor had been achieved in the transplanted HA mice. Relatively long-term cell survival (4 months post-transplant) was confirmed by co-staining with anti-HLA-ABC and anti-vWF antibodies as well as by the formation of blood vessels within the transplanted area (Figures 5B and 5C; Table S2).

Overall, these data indicate that corrected HA BOECs are able to engraft and persist for prolonged periods of time within the tissue matrix supported by the Cell Pouch and secrete enough FVIII to correct the hemophilia phenotype of the implanted NSG-HA mice.

Complex composition of BOEC clonal populations

Sonication linker-mediated PCR was performed on 53 samples of genomic DNA extracted from LV-transduced BOECs derived from 3 healthy donors (D45, D2, and D3) and 3 HA patients (pHA1, pA, and pC), collected at different expansion passages or procedure time points. By grouping the samples according to the BOEC source (i.e., healthy donors or HA patients) and the type of vector used (i.e., LV-VEC.hBDD-FVIII or LV-VEC.GFP), we obtained 4 main groups: HA.FVIII, HA.GFP, Healthy.FVIII, and Healthy.GFP. Overall, we retrieved 142,349 integration sites (ISs) (HA.FVIII, 28,069; HA.GFP, 106,554; Healthy.FVIII, 5,864; Healthy.GFP, 1,862) (Table S3). We compared the distribution of ISs of the four groups along the whole human genome and with respect to gene transcription start site. The profile of LV integrations was similar for all the groups and confirmed the marked tendency of the LV to integrate within gene bodies, without bias for promoter regions (Figures 6A and 6B), in line with previously published results.[53–56] Following enrichment analysis of genomic position and gene annotations, none of the ontological gene classes showed cancer or tumor suppressor gene enrichment (Table S4).

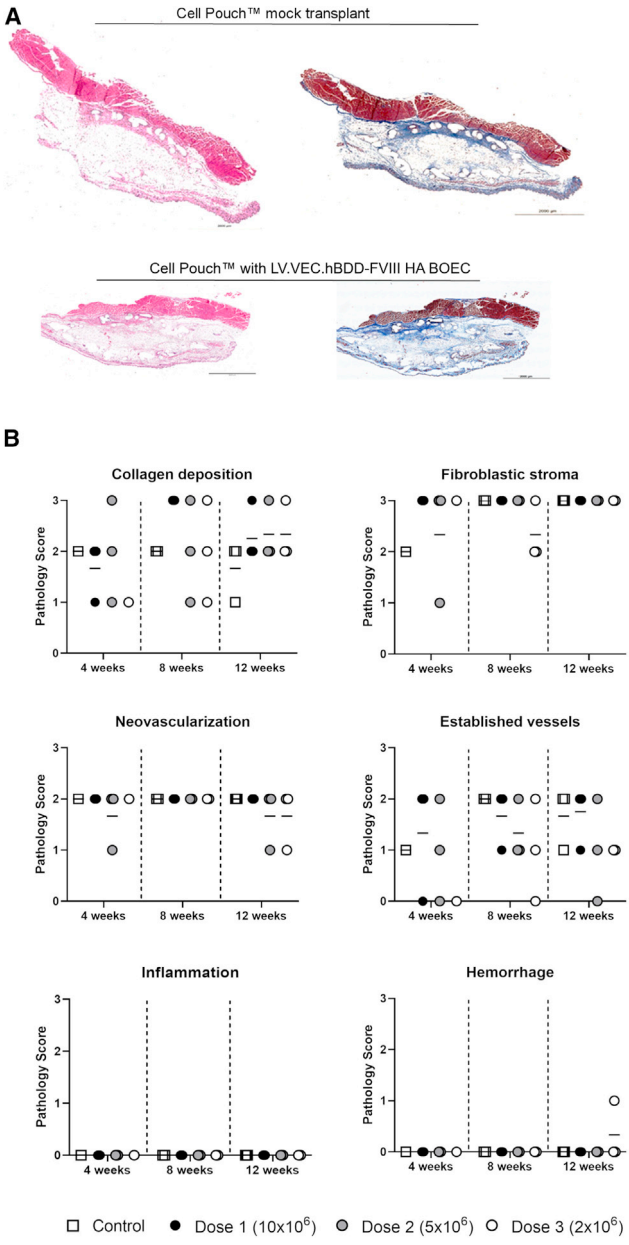

Figure 4. Pathological assessment after transplantation of LV-VEC.hBDD-FVIII HA BOECs into the Cell Pouch device

(A) Sernova Cell Pouches were removed at 4, 8, or 12 weeks and stained by H&E and Masson's trichrome for blinded histopathological analysis. Histology scores and representative images at 12 weeks post-transplant with 10 × 10^6 LV-VEC.hBDD-FVIII BOECs (animal groups n = 2–3). (B) Quantification of H&E and Masson's trichrome for blinded histopathological analysis.

Common insertion site (CIS) analysis showed few highly targeted genes in all datasets (e.g., *NPLOC4*, *PACS1*, and *MROH1*) (Table S5). The quantification of IS abundance showed only a few clones with abundance >10% in LV-VEC.hBDD-FVIII-transduced BOECs from pA and pHA1 (Figure 7). Only two ISs were retrieved from D45 cells transduced at an MOI of 30, thus resulting in both to be 50% abundant. One clone with an IS in the GNL3 gene, which may interact with p53 and may be involved in tumorigenesis, and with abundance >25%, was also observed in pHA1 BOEC, but only at a single time point (P11-UK). To address the clonality of transduced BOECs, we analyzed the diversity of the clonal population through Shannon diversity index. The highest Shannon diversity index, between 9 and 11, was observed in BOECs from pHA1 and pA, transduced with the VEC.GFP vector. All the other BOECs showed a Shannon diversity index between 4 and 8, which remained constant throughout the various cell passages. A lower diversity index directly correlated with a lower number of ISs, in particular for the HA Beads and Cell Pouch samples at different time points (Figure 8A). To better understand if, especially in the Cell Pouch samples, the clonal diversity was reduced, we compared the H index between samples grouped by type (expansion, HA beads, Cell Pouch and LV used [VEC-FVIII, VEC-GFP]) (Figure 8B). IS analysis revealed a high level polyclonality of LV-transduced BOECs, with no significant difference between the FVIII- and GFP-transduced samples. The clonal composition heterogeneity of FVIII-transduced samples remained constant over time *in vitro* and *in vivo*. Finally, Cell Pouch samples had a significant lower H index when compared with BOECs in expansion.

DISCUSSION

Although the current therapy for HA involves the administration of plasma-derived or recombinant FVIII, there is to date no definitive cure for this inherited bleeding disorder. While several ongoing phase I–III clinical trials assessing the feasibility and safety of AAV-mediated hepatocyte-directed HA gene therapy have been able to achieve therapeutic FVIII plasma levels,[57–59] further experiments are in progress to assess the long-term stability of transgene expression. In this regard, the fact that AAV vectors do not actively integrate into the host cell genome and, thus, can be lost upon cell division during liver growth or liver disease questions their life-long maintenance besides limiting their potential use in pediatric patients.

A promising alternative approach is represented by a combination of cell and gene therapy, which would, however, require the identification of a suitable cell type able to effectively secrete FVIII while meeting all the necessary conditions for successful cell transplantation. In this regard, it is widely acknowledged that the liver is the main organ producing FVIII, where LSECs appear to be the main source of FVIII[60–62] and can play a tolerogenic role. In addition, because of the important role of the interaction between FVIII and vWF in the stability and activity of FVIII, LSECs may represent the most suitable target for cell- and gene therapy-based strategies aimed to correct the HA phenotype.[63] Unfortunately, LSEC are not easy to obtain and maintain *in vitro*; therefore, in this study we explored the feasibility of using gene-corrected autologous BOECs more manageable and previously shown to be able to secrete FVIII *in vivo*.[64] Here, we show that BOECs isolated from both healthy and HA donors can be efficiently cultured, transduced, expanded, and used to correct the bleeding phenotype of HA mice. In this regard, it is important to

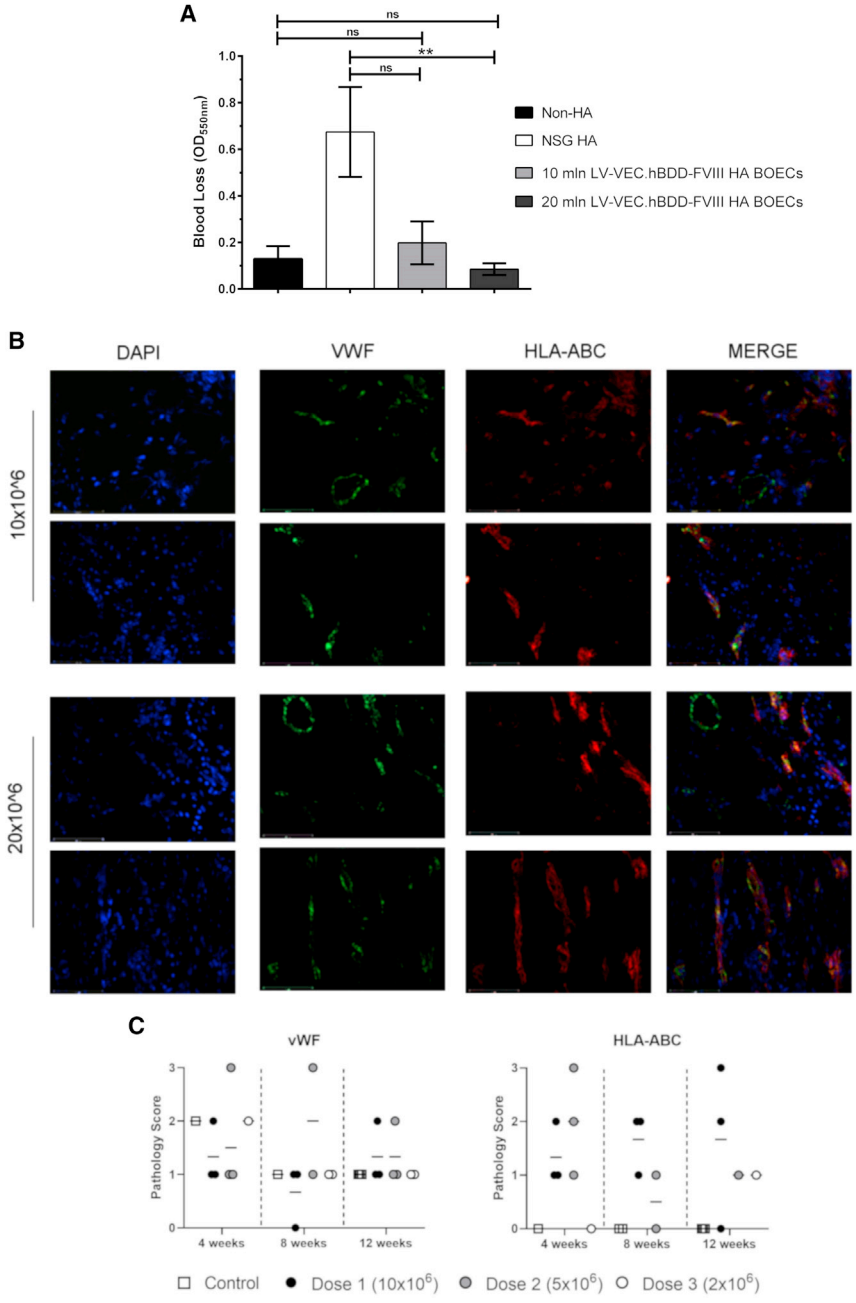

Figure 5. Bleeding phenotype and cell survival of LV-VEC.hBDD-FVIII HA BOECs after implantation in the Cell Pouch device

(A) Bleeding assay on mice transplanted with 10×10^6 or 20×10^6 HA and LV-VEC.hBDD-FVIII BOECs, or left untreated (n = 3–6, mean ± SEM, $^{**}p < 0.05$; ns, not significant). NSG mice were used as control for bleeding assay. (B) The transplanted Cell Pouch devices were removed from the recipient NSG-HA mice, and immunofluorescence was performed to detect cell survival within the mouse tissue by human cell staining (HLA-ABC) and blood vessel formation through staining with cross-reacting human/mouse von Willebrand factor (vWF) antibody. The images shown are representative of two transplant groups (10×10^6 n = 5; 20×10^6 n = 12). (C) Quantification of HLA-ABC and blood vessel formation from blinded histopathological assessment.

point out that the large number of corrected cells we obtained allowed us to reach FVIII therapeutic concentrations more quickly, thus reducing the risk of cell senescence.

The current protocols for BOEC isolation are based on the culture of mononuclear cells (MNCs) from peripheral or umbilical cord blood on collagen-coated cell culture vessels in endothelial-specific medium.[65] The fact that MNCs can be isolated directly through density gradient centrifugation of blood makes these cells a safe cell source for hemophilic patients. Normally, BOEC colonies arise after 2–4 weeks of culture, and the colonies are very rare since their number in the normal peripheral blood is quite low.[65] However, here we show that, under GMP-compliant conditions and using a chemically defined medium, it is possible to isolate BOECs from both healthy donors and HA patients with high efficiency and rapidly grow them to the desired amount to prevent the risk of cellular senescence once transplanted in mice.

In addition to being more easily obtainable, BOECs are fully differentiated ECs with a mature endothelial phenotype. Indeed, these cells originate from bone marrow-derived progenitors circulating in the blood or residing in the endothelium, which can be differentiated into BOECs *in vitro*.[66] Thus, the observation that the expanded pools of BOECs from healthy donors or HA patients retained the expression of endothelial markers and were able to form vessels indicates that our GMP-compliant conditions did not alter the endothelial phenotype and function of these cells, as shown previously.[66] Moreover, the healthy BOECs showed low FVIII expression, as demonstrated by IF staining and FACS analysis, in agreement with the low FVIII secretion found in the cell supernatant. This is similar to what has been shown by previous studies in which healthy BOECs isolated from both canine and human donors displayed low FVIII expression.[41,50,51] Indeed, FVIII expression heterogeneity among different endothelial subpopulations has been reported, with the sinusoidal ECs shown as the main FVIII-secreting cells.[67] Another important aspect of this study is that we efficiently transduced BOECs with an LV carrying a functional BDD form of FVIII driven by the endothelial-specific promoter VEC. The efficiency and tissue specificity of FVIII transcription under the control of this promoter has been previously

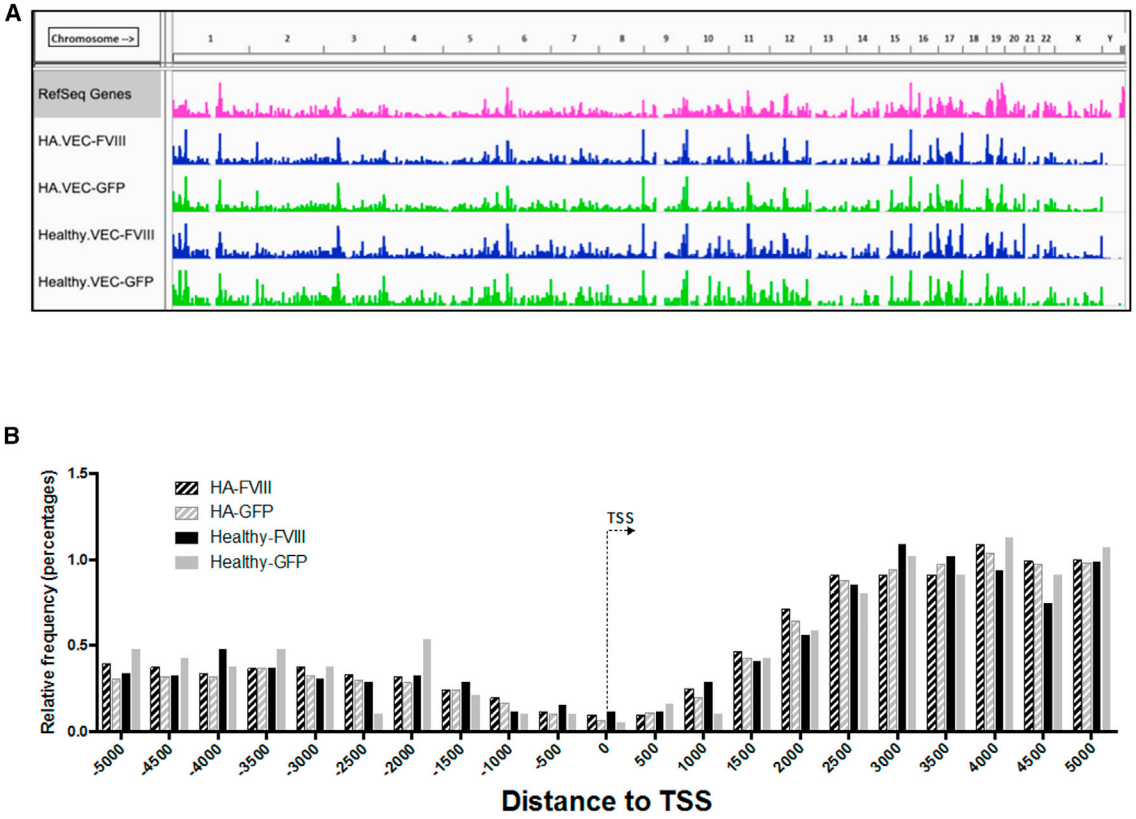

Figure 6. Genome wide distribution of lentiviral vector ISs

(A) The pink track represents the density distribution of genes (RefSeq annotation, hg19 genome). The green tracks are the density distributions of all the ISs retrieved in the HA transduced with LV-VEC.GFP and Healthy transduced with LV-VEC.GFP groups. The blue tracks are the density distributions of all the ISs retrieved in the LV-VEC.hBDD-FVIII HA BOECs and LV-VEC.hBDD-FVIII Healthy BOECs groups. (B) Distribution of ISs of the four groups along the whole human genome and with respect to gene transcription start site (TSS).

demonstrated in gene therapy approaches showing the restriction of FVIII expression in the desired cell type[68] and in cell therapy by secretion of FVIII after genetic correction in target cells.[31] Here, we show that LV-corrected HA BOECs transplanted in association with Cytodex 3 microcarrier beads into the peritoneum of NSG-HA mice rescues the hemophilic phenotype of these animals for up to 18 weeks, achieving 9% FVIII activity.

Importantly, we reached therapeutic levels of secreted FVIII through LV-VEC.hBDD-FVIII HA BOEC injection into a prevascularized Cell Pouch device transplanted into a preclinical murine model of severe HA. Notably, the correction of the bleeding phenotype by using LV-VEC.hBDD-FVIII HA BOECs injected into the peritoneum lasted up to 13 weeks and then slowly decreased. After 18 weeks, FVIII activity was almost absent, probably due to the death of BOECs.

Despite the encouraging results presented in this proof-of-concept study in a preclinical setting, there still remain several important issues that need to be addressed before our approach can be brought into the clinic. For instance, it will be imperative to characterize the cells within the Cell Pouch in terms of cell markers, longevity, and proliferation/senescence status. It will also be important to assess if we can increase the expression levels of FVIII using different EC-specific promoters, and if that would translate into augmented FVIII secretion and functionality *ex vivo*.

Overall, our findings indicate that cell transfer into a medical device is a suitable solution for cell therapy as it confers a more physiological and protected environment where cells can proliferate at an excellent rate and escape from the immune response of the transplanted organism, all the while allowing nutrient exchange and therapeutic protein secretion. Congruently, the safety and efficacy of the Cell Pouch for the transplantation of mouse pancreatic islets has been previously shown to provide insulin independence in diabetic animals in preclinical studies of type 1 diabetes mellitus.[45,69] Furthermore, a phase I/II clinical trial is ongoing for the treatment of T1DM patients, the result of which may support the potential application of this device to other diseases for cell therapy approaches, such as HA.[70]

The Cell Pouch is a biocompatible, safe, implantable device that forms an internal vascularized tissue matrix supporting the transplanted cells. When we analyzed the Cell Pouch injected with

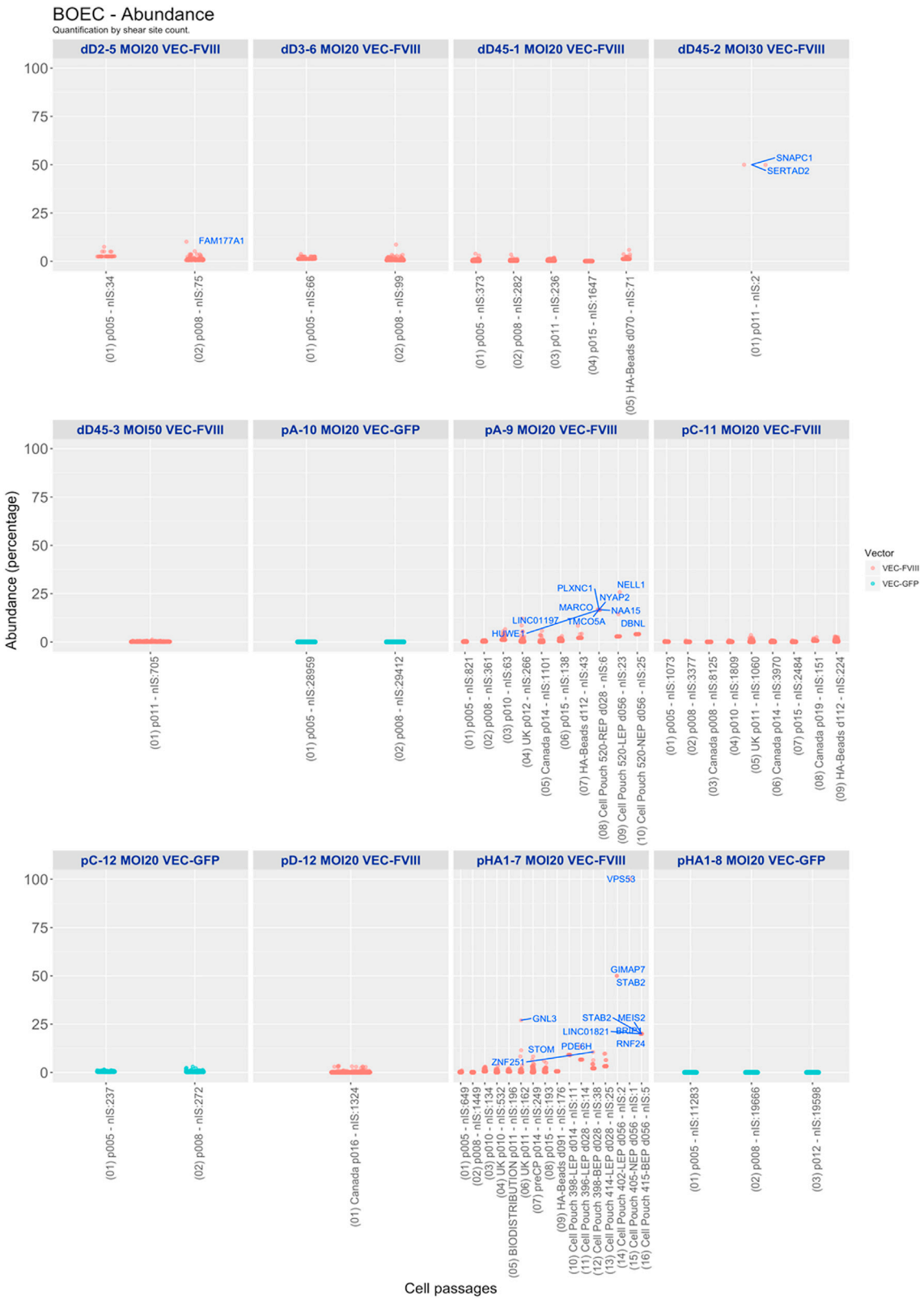

Figure 7. Boxplot representation of clonal abundance

For each sample, the abundance values for each clone are represented as dots. Clones over 10% are presented as dots labeled with the closest gene symbol (RefSeq hg19).

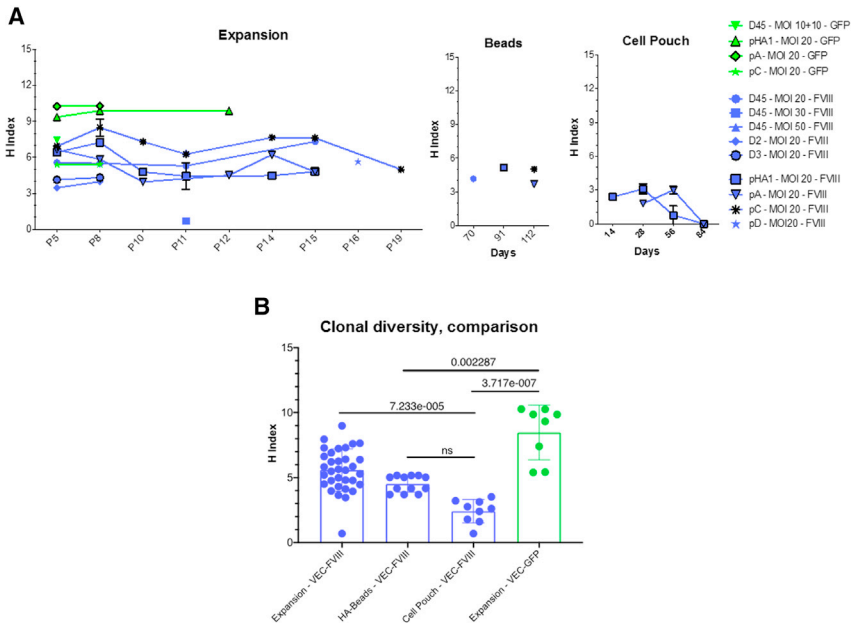

Figure 8. Clonal diversity comparison

(A) Shannon diversity index for each transduced cell population according to cell passage and time point. (B) H index comparison between different groups.

LV-VEC.hBDD-FVIII HA BOECs after 4 weeks from cell transfer, we observed the presence of a viable vascularized tissue matrix supporting the cells, with no evidence of fibrosis-associated consequences, including inflammation and necrosis, or hemophilia-related hemorrhage episodes. Moreover, the bleeding assay demonstrated that LV-VEC.FVIII HA BOECs transplanted into the vascularized subcutaneous Cell Pouch were able to correct the clotting function of HA mice. FVIII secretion and activity measurement would support the data on hemophilic correction and strengthen our observations. These tests are planned for future studies. As previously shown in a canine model of HA, BOECs transduced with an LV carrying the canine FVIII and implanted subcutaneously allowed secretion of therapeutic levels of FVIII up to 15 weeks in Matrigel scaffolds and up to a year after omental implantation.[64] Moreover, BOECs were shown to form tubule networks *in vitro* when plated on Matrigel[71] or on the surface of synthetic vascular scaffolds[72] and to promote neovascularization *in vivo* when transplanted into immunodeficient mice,[37] suggesting that they can be directly involved in vessel formation.

In this context, our data attest the feasibility of a method to correct autologous cells based on a combined cell and gene therapy approach together with the use of a scaffold (i.e., Cell Pouch) able to guarantee long-term cell survival and, in case of need, a re-injection of new therapeutic cells. In addition to the phenotypical and functional characterization of the transduced HA BOECs, our results demonstrate the pharmacodynamics proof-of-concept in non-clinical models, which is mandatory before any GTMP can be used in human clinical trial.[43,44] Thus, our next step will be to evaluate the safety and toxicity of the GTMP *in vivo* based on these results so as to ensure patient safety and promote product translation. Examples of required non-clinical studies are the evaluation of the potential tumorigenicity and biodistribution of the transduced BOECs with or without the medical device.[73] Our molecular analysis of the integration sites in BOECs shows that no enrichment for oncogenes or expansion of clones with ISs in CISs or biases toward gene classes related to cancer genes occurred. IS analysis suggests a high level of polyclonality of LV-transduced BOECs, with no statistical difference between the FVIII- and GFP-transduced samples. The heterogeneity of the clonal composition of the FVIII-transduced samples remained constant over time (between different cell passages) also when cells were coupled to the microcarrier beads. Furthermore, Cell Pouch samples had a statistically significant lower H index when compared with BOECs in expansion.

The process of BOEC engraftment within the subcutaneous space is novel and complex and further studies will provide additional insight into the interactions between the developing tissue and the transplanted cells, elucidating the role played in the kinetics of blood vessel formation and FVIII secretion within the surrounding tissue.

In this study, we could not evaluate the immune response to the secreted factor because we used implanted cells in immunodeficient hemophilic mice. Thus, in future studies it will be interesting to evaluate antibody formation after transplantation of transduced BOECs encapsulated in the Cell Pouch into immunocompetent mice. Finally, while several gene therapy clinical trials for HA are ongoing, to our knowledge this is the first therapeutic approach that combines the GMP production of autologous human BOECs with the use of a safe *ex vivo* approach based on an implantable prevascularized device.

In conclusion, our findings suggest that long-term encapsulation and survival of LV-corrected BOECs by means of an implantable device may prove effective in ameliorating the QoL of HA patients. The therapeutic dose of FVIII released by these autologous genetically modified cells would in fact prevent the need of frequent infusions of FVIII and significantly reduce the morbidity and the frequency of the bleeding episodes in hemophiliacs.

MATERIALS AND METHODS

BOEC isolation form HA patients and healthy donors

Blood sampling from four adult severe HA patients, named pHA1, pA, pC, and pD, was performed at the hospital A.O.U. Città della Salute e della Scienza, Turin, Italy. The blood was shipped at

room temperature to Università del Piemonte Orientale (UPO), Novara, Italy. Blood sampling from adult severe HA patients was approved by the Ethics Committee "Comitato Etico Interaziendale A.O.U. Maggiore della Carità" (Protocol 810/CE, study no. CE 125/17). Human BOECs were isolated as described previously,[65] with the introduction of an earlier cell passaging step 7 days after initial isolation of the peripheral blood MNCs to reduce expansion time and increase the final cell yield.[74] Isolated cells were cultured on CELLCOAT Collagen Type 1-coated tissue culture flasks (Greiner Bio-One) using MCDB 131 medium (Gibco, Life Technologies) containing proprietary supplements. Primary cells from adult healthy donors (named D45, D2, and D3) were isolated at Tissue Engineering and Regenerative Medicine, Würzburg, Germany, under informed consent according to ethical approval granted by the Institutional Ethics Committee of the University Hospital Würzburg (approval no. 182/10). Cell viability and count were assessed using the Countess II FL Automated Cell Counter (Thermo Fisher Scientific).

Healthy and HA BOEC transduction

Healthy and HA BOECs were plated at a 10^4 cells/cm^2 density and after 6–8 h transduced with a lentiviral vector carrying the BDD form of FVIII under the control of the VE-cadherin promoter (LV-VEC.hBDD-FVIII) or with a lentiviral vector carrying the green fluorescent protein under the control of the same VE-cadherin promoter (LV-VEC.GFP), using an MOI of 20. After 14–16 h incubation, fresh medium was added to the cells and, 72 h later, half of the cells were harvested for subsequent analysis, while the other half was further cultured.

GMP-compliant (GMP-like) preclinical development of LV-VEC.hBDD-FVIII-transduced BOECs

BOECs were isolated and expanded using a GMP-compliant standardized approach between all partners, including a quality control strategy. The standardized expansion scheme defined within the project is based on the generation of Master Cell Banks and a Working Cell Bank, which ensures not only a controllable defined expansion for each patient's BOECs but also an in-process quality control at defined crucial steps. After isolation and expansion, cells were transduced with LV lots produced with a GMP-compliant method (TFF, see supplemental information). All freezing steps were performed using a cryopreservation solution based on compounds that are GMP-compliant free of toxic compounds (e.g., DMSO). The Cell Pouch was manufactured under GMP-compliant conditions. All steps were designed and conducted according to European GMP regulations to ensure that the product would fully comply with the quality requirements of the European authorities. The main objectives were to provide sets of design and manufacturing protocols based on current European GMP regulations and to prepare an Investigational Medicinal Product Dossier for an Investigational Medicinal Product, composed of therapeutic cells and an implantable medical device (Cell Pouch), a so-called combined Advanced Therapeutic Medicinal Product (combined ATMP).

IS analysis

ISs were retrieved from genomic DNA of LV-transduced BOEC cells by sonication linker-mediated PCR, an adaptation of a previously described method.[75,76] Genomic DNA (300 ng) was sheared using a Covaris E220 Ultrasonicator (Covaris, Woburn, MA), generating fragments with a target size of 1,000 bp. The fragmented DNA was split into three parts to generate technical replicates and, by using the NEBNext Ultra DNA Library Prep Kit for Illumina (New England Biolabs, Ipswich, MA), subjected to end repair, 3′ adenylation, and ligation to linker cassettes (Integrated DNA Technologies, Skokie, IL) containing an 8-nucleotide sequence barcode used for sample identification and a 12-random nucleotide sequence necessary for clonal abundance quantification. Ligation products were then subjected to 35 cycles of exponential PCR using primers specific for the lentiviral vector LTR and the linker cassette. The amplification product was then re-amplified with an additional 10 PCR cycles using primers specific for the linker cassette and the LTR, with the latter containing a second barcode to adopt a double barcode strategy for sample identification. The final PCR products were quantified using a KAPA Library Quantification Kit (Roche, Basil, Switzerland) and pooled in sequencing libraries with equimolar composition, avoiding repeated barcode pairs. Primers incorporate the adapter sequences required for the Illumina paired end sequencing technology (Illumina, San Diego, CA). Sequencing was performed on the Illumina MiSeq and HiSeq. Sample processing and metadata were tracked within our laboratory information management system.[77,78] Sequencing reads were processed using a dedicated bioinformatics pipeline (VISPA2).[78] In brief, paired sequence reads were filtered for raw read quality, then cleaned by vector genome, and the resulting cellular genomic sequence mapped on the human genome (version hg19), and the nearest RefSeq gene assigned to each unambiguously mapped ISs. Clonal abundance for each IS was estimated using the R package sonicLength,[79] where the number of genomes with the same integration site is calculated by counting the number of fragments with different sizes generated by sonication belonging to each individual IS. Within each group, ISs shared between different time points of the same transduction were counted once. The relative abundance of each clone was then calculated as the percentage of genomes with a specific integration site over the total genomes. CISs were identified through the Grubbs test for outliers.[80] Enrichment analysis for ontological classes among the targeted genes by vector ISs was performed using the Genomic Regions Enrichment of Annotations Tool.[81]

Animal procedures

Animal studies were approved by the Animal Care and Use Committee at UPO (Italian Health Ministry Authorization nos. 492/2016-PR and DBO64.5). NOD.Cg-Prkdc^{scid}Il2rg^{tm1Wjl}/SzJ (Jackson, stock no. 005557) mice with hemophilic phenotype (NSG-HA) were previously generated and maintained in our laboratory.[22] Eight- to 10-week-old animals were used for cell transplantation studies. Cell Pouch implantations were conducted under additional ethical guidelines and approval from the Animal Care Committee at the University of British Columbia (Vancouver, BC, Canada) in accordance with the

Canadian Council on Animal Care Guide to the Care and Use of Experimental Animals.

BOEC transplantation

For cell transplantation with beads, 5×10^6 FVIII-transduced healthy or HA BOECs were mixed with Cytodex 3 microcarrier beads (GE Healthcare Life Sciences) and intraperitoneally delivered in NSG-HA mice as described previously.[23] For Cell Pouch implantation, female NSG and NSG-HA animals were anesthetized and surgically implanted with a Cell Pouch in the subcutaneous space of the lower abdomen 4 weeks before cell transplantation, allowing incorporation with vascularized tissue and forming fully developed tissue chambers suitable for cell transplantation upon removal of a space holding plug. LV-VEC.hBDD-FVIII BOECs were cultured for 3 days post-thawing and finally transplanted into the Cell Pouch. Mice received either a dose of viable BOECs ($2–20 \times 10^6$) or remained untreated. All animals received a prophylactic dose (2–4 IU) of recombinant human FVIII by tail vein injection before surgical procedures.

FVIII activity

aPTT assay was performed on plasma samples of transplanted mice to assess FVIII activity. Standard curves were generated by serial dilution of recombinant human BDD-FVIII (ReFacto) in hemophilic mouse plasma. Analyses were performed using a Coatron M4 coagulometer (TECO Medical Instruments) and TEClot APTT-S kit reagents (TECO Medical Instruments).

Bleeding assay

A bleeding assay was performed on anesthetized mice. The distal portion of the tail was cut at a diameter of 2–2.5 mm. Tails were placed in a conical tube containing 14 mL of 37°C pre-warmed saline. Blood was collected for 10 min and, following centrifugation, resuspended in red blood lysis buffer (155 mM NH_4Cl, 10 mM $KHCO_3$, and 0.1 mM EDTA). The absorbance of the samples was measured at 575 nm. For cell transplantation experiments with Cell Pouch, the tail bleeding assay was performed using Sernova, as described previously,[82,83] at the end of the experimental period, 4 months post-transplantation. In brief, mice were anesthetized, and tail tips were placed in a guide, ensuring the same diameter of 1 mm, and severed (~a distal 10-mm segment) for each animal. The tail was immediately immersed in pre-warmed saline at 37°C. Bleeding was carried out for a maximum of 20 min, after which animals were euthanized as per approved animal use protocols. Blood loss was evaluated by determining hemoglobin concentration by lysing collected red blood cells (ACK Lysing Buffer, Gibco), and the absorbance measured at 550 nm on a Synergy Mx (BioTeck) spectrophotometer. Results were analyzed by comparing the amount of blood loss obtained from treated NSG-HA mice with control mice (untreated NSG-HA and NSG mice).

Statistical analysis

Data were expressed as means ± standard deviation (SD) or means ± standard error of the mean (SEM). Statistical significance was analyzed using Student's t test with two-tailed distribution, assuming equal SD distribution, two-way analysis of variance with Bonferroni post hoc test, or Tukey's multiple comparison post hoc tests in GraphPad Prism 6 (GraphPad software). Statistical analyses involving ISs were performed with the R software (r-project.org). Differences were considered statistically significant when p values were <0.05.

SUPPLEMENTAL INFORMATION

Supplemental information can be found online at https://doi.org/10.1016/j.omtm.2021.10.015.

ACKNOWLEDGMENTS

The authors thank Dr. D. Burton and Dr. A. Iftimia-Mander for their help, and V. Bruscaggin and V. Fiorio for technical assistance. We also thanks Dr. Marcello Arsura for the English revision of the manuscript. A.F., M.Z., A.S., P.M.T., and J.B. have received funding from the European Union's Horizon 2020 research and innovation program under grant agreement HemAcure no. 667421. A.F. was also supported in part by Telethon grant no. GGP19201 and by Horizon 2020, Vanguard grant no. 874700. This study was also partially funded by the Università del Piemonte Orientale (FAR 2017) to S.M., Fondazione Cariplo grant no. 2018-0253 to C.B., and by Italian Minister of Health "Ricerca Sanitaria finalizzata" Giovani Ricercatori grant no. 2018-12366399 to C.O.

AUTHOR CONTRIBUTIONS

C.O., C.B., S.M., T.B., P.B., A.B.A., N.W., K.P. and A. Cucci. performed the research and analyzed the data. A. Calabria, F.B., and E.M. performed integration analysis and analyzed the data. A.B. and B.P. collected blood samples from hemophilic patients and performed analysis. A.F., J.B., A.S., D.M.M., P.M.T., and M.Z. conceived the experiments generated funding, designed the research, and analyzed the data. C.O., C.B., S.M., and A.F. wrote the manuscript that was revised by all authors.

DECLARATION OF INTERESTS

K.P., D.M.M., and P.M.T. are/have been employees of Sernova Corp., which holds the patent US20190240375A1.

REFERENCES

1. Bolton-Maggs, P.H.B., and Pasi, K.J. (2003). Haemophilias A and B. In Lancet, pp. 1801–1809.
2. Roth, D.A., Tawa, N.E., O'Brien, J.M., Treco, D.A., and Selden, R.F. (2001). Nonviral transfer of the gene encoding coagulation factor VIII in patients with severe hemophilia A. N. Engl. J. Med. *344*, 1735–1742.
3. Lissitchkov, T., Rusen, L., Georgiev, P., Windyga, J., Klamroth, R., Gercheva, L., Nemes, L., Tiede, A., Bichler, J., Knaub, S., et al. (2017). PK-guided personalized prophylaxis with Nuwiq® (human-cl rhFVIII) in adults with severe haemophilia A. Haemophilia *23*, 697–704.
4. Saxena, K., Lalezari, S., Oldenburg, J., Tseneklidou-Stoeter, D., Beckmann, H., Yoon, M., and Maas Enriquez, M. (2016). Efficacy and safety of BAY 81-8973, a full-length recombinant factor VIII: results from the LEOPOLD I trial. Haemophilia *22*, 706–712.
5. Mahlangu, J., Kuliczkowski, K., Karim, F.A., Stasyshyn, O., Kosinova, M.V., Lepatan, L.M., Skotnicki, A., Boggio, L.N., Klamroth, R., Oldenburg, J., et al. (2016). Efficacy and safety of rVIII-singlechain: results of a phase 1/3 multicenter clinical trial in severe hemophilia A. Blood *128*, 630–637.

6. Lentz, S.R., Janic, D., Kavakli, K., Miljic, P., Oldenburg, J., Ozelo, C.M., Santagostino, E., Suzuki, T., Zupancic Šalek, S., et al. (2018). Long-term safety and efficacy of turoctocog alfa in prophylaxis and treatment of bleeding episodes in severe haemophilia A: final results from the guardian 2 extension trial. Haemophilia *24*, e391–e394.

7. Mahlangu, J., Young, G., Hermans, C., Blanchette, V., Berntorp, E., and Santagostino, E. (2018). Defining extended half-life rFVIII—a critical review of the evidence. Haemophilia *24*, 348–358.

8. Mahlangu, J., Powell, J.S., Ragni, M.V., Chowdary, P., Josephson, N.C., Pabinger, I., Hanabusa, H., Gupta, N., Kulkarni, R., Fogarty, P., et al. (2014). Phase 3 study of recombinant factor VIII Fc fusion protein in severe hemophilia A. Blood *123*, 317–325.

9. Konkle, B.A., Stasyshyn, O., Chowdary, P., Bevan, D.H., Mant, T., Shima, M., Engl, W., Dyck-Jones, J., Fuerlinger, M., Patrone, L., et al. (2015). Pegylated, full-length, recombinant factor VIII for prophylactic and on-demand treatment of severe hemophilia A. Blood *126*, 1078–1085.

10. Cormier, M., Batty, P., Tarrant, J., and Lillicrap, D. (2020). Advances in knowledge of inhibitor formation in severe haemophilia A. Br. J. Haematol. *189*, 39–53.

11. Dimichele, D. (2002). Inhibitors: resolving diagnostic and therapeutic dilemmas. Haemophilia *8*, 280–287.

12. Van Den Berg, H.M., Fischer, K., Carcao, M., Chambost, H., Kenet, G., Kurnik, K., Königs, C., Male, C., Santagostino, E., and Ljung, R. (2019). Timing of inhibitor development in more than 1000 previously untreated patients with severe hemophilia A. Blood *134*, 317–320.

13. Oldenburg, J., Mahlangu, J.N., Kim, B., Schmitt, C., Callaghan, M.U., Young, G., Santagostino, E., Kruse-Jarres, R., Negrier, C., Kessler, C., et al. (2017). Emicizumab prophylaxis in hemophilia A with inhibitors. N. Engl. J. Med. *377*, 809–818.

14. Pipe, S.W., Shima, M., Lehle, M., Shapiro, A., Chebon, S., Fukutake, K., Key, N.S., Portron, A., Schmitt, C., Podolak-Dawidziak, M., et al. (2019). Efficacy, safety, and pharmacokinetics of emicizumab prophylaxis given every 4 weeks in people with haemophilia A (HAVEN 4): a multicentre, open-label, non-randomised phase 3 study. Lancet Haematol. *6*, e295–e305.

15. Ebbert, P.T., Xavier, F., Seaman, C.D., and Ragni, M.V. (2020). Emicizumab prophylaxis in patients with haemophilia A with and without inhibitors. Haemophilia *26*, 41–46.

16. Zimowski, K.L., Batsuli, G.M., Bryant, P., McDaniel, J., Tickle, K., Meeks, S.L., and Sidonio, R.F. (2019). Severe bleeding events in hemophilia A patients receiving emicizumab prophylaxis. Blood *134*, 1126.

17. Wion, K.L., Kelly, D., Summerfield, J.A., Tuddenham, E.G.D., and Lawn, R.M. (1985). Distribution of factor VIII MRNA and antigen in human liver and other tissues. Nature *317*, 726–729.

18. Jiang, H.C., Gao, Y., Dai, W.J., Sun, B., Xu, J., Qiao, H.Q., Meng, Q.H., and Wu, C.J. (2006). Ten-year experience with living related donated splenic transplantation for the treatment of hemophilia. A. Transpl. Proc. *38*, 1483–1490.

19. Hollestelle, M.J., Thinnes, T., Crain, K., Stiko, A., Kruijt, J.K., Van Berkel, T.J.C., Loskutoff, D.J., and Van Mourik, J.A. (2001). Tissue distribution of factor VIII gene expression in vivo—a closer look. Thromb. Haemost. *86*, 855–861.

20. Hollestelle, M.J., Poyck, P.P.C., Hollestelle, J.M., Marsman, H.A., Van Mourik, J.A., and Van Gulik, T.M. (2005). Extra-hepatic factor VIII expression in porcine fulminant hepatic failure. J. Thromb. Haemost. *3*, 2274–2280.

21. Follenzi, A., Raut, S., Merlin, S., Sarkar, R., and Gupta, S. (2012). Role of bone marrow transplantation for correcting hemophilia A in mice. Blood *119*, 5532–5542.

22. Zanolini, D., Merlin, S., Feola, M., Ranaldo, G., Amoruso, A., Gaidano, G., Zaffaroni, M., Ferrero, A., Brunelleschi, S., Valente, G., et al. (2015). Extrahepatic sources of factor VIII potentially contribute to the coagulation cascade correcting the bleeding phenotype of mice with hemophilia A. Haematologica *100*, 881–892.

23. Kumaran, V., Benten, D., Follenzi, A., Joseph, B., Sarkar, R., and Gupta, S. (2005). Transplantation of endothelial cells corrects the phenotype in hemophilia A mice. J. Thromb. Haemost. *3*, 2022–2031.

24. Fomin, M.E., Zhou, Y., Beyer, A.I., Publicover, J., Baron, J.L., and Muench, M.O. (2013). Production of factor VIII by human liver sinusoidal endothelial cells transplanted in immunodeficient uPA mice. PLoS One *8*, e77255.

25. Follenzi, A., Benten, D., Novikoff, P., Faulkner, L., Raut, S., and Gupta, S. (2008). Transplanted endothelial cells repopulate the liver endothelium and correct the phenotype of hemophilia A mice. J. Clin. Invest. *118*, 935–945.

26. Filali, E. El, Hiralall, J.K., Van Veen, H.A., Stolz, D.B., and Seppen, J. (2013). Human liver endothelial cells, but not macrovascular or microvascular endothelial cells, engraft in the mouse liver. Cell Transpl. *22*, 1801–1811.

27. Gollomp, K.L., Doshi, B.S., and Arruda, V.R. (2019). Gene therapy for hemophilia: progress to date and challenges moving forward. Transfus. Apher. Sci. *58*, 602–612.

28. Peyvandi, F., and Garagiola, I. (2019). Clinical advances in gene therapy updates on clinical trials of gene therapy in haemophilia. Haemophilia *25*, 738–746.

29. Samelson-Jones, B.J., and Arruda, V.R. (2020). Translational potential of immune tolerance induction by AAV liver-directed factor VIII gene therapy for hemophilia A. Front. Immunol. *11*, 618.

30. Merlin, S., Famà, R., Borroni, E., Zanolini, D., Bruscaggin, V., Zucchelli, S., and Follenzi, A. (2019). FVIII expression by its native promoter sustains long-term correction avoiding immune response in hemophilic mice. Blood Adv. *3*, 825–838.

31. Olgasi, C., Talmon, M., Merlin, S., Cucci, A., Richaud-Patin, Y., Ranaldo, G., Colangelo, D., Di Scipio, F., Berta, G.N., Borsotti, C., et al. (2018). Patient-specific iPSC-derived endothelial cells provide long-term phenotypic correction of hemophilia A. Stem Cell Reports *11*, 1391–1406.

32. Gao, K., Kumar, P., Cortez-Toledo, E., Hao, D., Reynaga, L., Rose, M., Wang, C., Farmer, D., Nolta, J., Zhou, J., et al. (2019). Potential long-term treatment of hemophilia A by neonatal co-transplantation of cord blood-derived endothelial colony-forming cells and placental mesenchymal stromal cells. Stem Cell Res. Ther. *10*, 3318.

33. Park, C.-Y., Kim, D.H., Son, J.S., Sung, J.J., Lee, J., Bae, S., Kim, J.-H., Kim, D.-W., and Kim, J.-S. (2015). Functional correction of large factor VIII gene chromosomal inversions in hemophilia A patient-derived iPSCs using CRISPR-cas9. Cell Stem Cell *17*, 213–220.

34. Tatsumi, K., Sugimoto, M., Lillicrap, D., Shima, M., Ohashi, K., Okano, T., and Matsui, H. (2013). A novel cell-sheet technology that achieves durable factor VIII delivery in a mouse model of hemophilia A. PLoS One *8*, e83280.

35. Lin, Y., Weisdorf, D.J., Solovey, A., and Hebbel, R.P. (2000). Origins of circulating endothelial cells and endothelial outgrowth from blood. J. Clin. Invest. *105*, 71–77.

36. Yoder, M.C., Mead, L.E., Prater, D., Krier, T.R., Mroueh, K.N., Li, F., Krasich, R., Temm, C.J., Prchal, J.T., and Ingram, D.A. (2007). Redefining endothelial progenitor cells via clonal analysis and hematopoietic stem/progenitor cell principals. Blood, 1801–1809.

37. Hoshi, R.A., Van Lith, R., Jen, M.C., Allen, J.B., Lapidos, K.A., and Ameer, G. (2013). The blood and vascular cell compatibility of heparin-modified ePTFE vascular grafts. Biomaterials *34*, 30–41.

38. Melero-Martin, J.M., Khan, Z.A., Picard, A., Wu, X., Paruchuri, S., and Bischoff, J. (2007). In vivo vasculogenic potential of human blood-derived endothelial progenitor cells. Blood *109*, 4761–4768.

39. Jantzen, A.E., Lane, W.O., Gage, S.M., Jamiolkowski, R.M., Haseltine, J.M., Galinat, L.J., Lin, F.H., Lawson, J.H., Truskey, G.A., and Achneck, H.E. (2011). Use of autologous blood-derived endothelial progenitor cells at point-of-care to protect against implant thrombosis in a large animal model. Biomaterials *32*, 8356–8363.

40. Sarlon, G., Zemani, F., David, L., Duong van Huyen, J.P., Dizier, B., Grelac, F., Colliec-Jouault, S., Galy-Fauroux, I., Bruneval, P., Fischer, A.M., et al. (2012). Therapeutic effect of fucoidan-stimulated endothelial colony-forming cells in peripheral ischemia. J. Thromb. Haemost. *10*, 38–48.

41. Lin, Y., Chang, L., Solovey, A., Healey, J.F., Lollar, P., and Hebbel, R.P. (2002). Use of blood outgrowth endothelial cells for gene therapy for hemophilia A. Blood *99*, 457–462.

42. Medicines Agency, E.. (2015). Reflection Paper on Classification of Advanced Therapy Medicinal Products, https://www.ema.europa.eu/en/documents/scientific-guideline/reflection-paper-classification-advanced-therapy-medicinal-products_en-0.pdf.

43. Medicines Agency, E.. (2020). Guideline on Quality, Non-clinical and Clinical Aspects of Medicinal Products Containing Genetically Modified Cells, https://www.ema.europa.eu/en/documents/scientific-guideline/guideline-quality-non-clinical-clinical-aspects-medicinal-products-containing-genetically-modified_en-0.pdf.

44. Medicines Agency, E.. (2008). Guideline on the Non-clinical Studies Required before First Clinical Use of Gene Therapy Medicinal Products, https://www.ema.europa.eu/en/documents/scientific-guideline/guideline-non-clinical-studies-required-first-clinical-use-gene-therapy-medicinal-products_en.pdf.

45. Pepper, A.R., Pawlick, R., Gala-Lopez, B., MacGillivary, A., Mazzuca, D.M., White, D.J.G., Toleikis, P.M., and James Shapiro, A.M. (2015). Diabetes is reversed in a murine model by marginal mass syngeneic islet transplantation using a subcutaneous cell pouch device. Transplantation *99*, 2294–2300.

46. Charrier, S., Ferrand, M., Zerbato, M., Précigout, G., Viornery, A., Bucher-Laurent, S., Benkhelifa-Ziyyat, S., Merten, O.W., Perea, J., and Galy, A. (2011). Quantification of lentiviral vector copy numbers in individual hematopoietic colony-forming cells shows vector dose-dependent effects on the frequency and level of transduction. Gene Ther. *18*, 479–487.

47. Zhao, Y., Stepto, H., and Schneider, C.K. (2017). Development of the first World Health Organization lentiviral vector standard: toward the production control and standardization of lentivirus-based gene therapy products. Hum. Gene Ther. Methods *28*, 205–214.

48. Furuhata, S., Ando, K., Oki, M., Aoki, K., Ohnishi, S., Aoyagi, K., Sasaki, H., Sakamoto, H., Yoshida, T., and Ohnami, S. (2007). Gene expression profiles of endothelial progenitor cells by oligonucleotide microarray analysis. Mol. Cell. Biochem. *298*, 125–138.

49. Nelson, G.M., Padera, T.P., Garkavtsev, I., Shioda, T., and Jain, R.K. (2007). Differential gene expression of primary cultured lymphatic and blood vascular endothelial cells. Neoplasia *9*, 1038–1045.

50. Matsui, H., Shibata, M., Brown, B., Labelle, A., Hegadorn, C., Andrews, C., Hebbel, R.P., Galipeau, J., Hough, C., and Lillicrap, D. (2007). Ex vivo gene therapy for hemophilia A that enhances safe delivery and sustained in vivo factor VIII expression from lentivirally engineered endothelial progenitors. Stem Cells *25*, 2660–2669.

51. Biggelaar, M.van den, Bouwens, E.A.M., Kootstra, N.A., Hebbel, R.P., Voorberg, J., and Mertens, K. (2009). Storage and regulated secretion of factor VIII in blood outgrowth endothelial cells. Haematologica *94*, 670–678.

52. Nielsen, J.S., and Mcnagny, K.M. (2008). Novel functions of the CD34 family. J. Cell Sci. *121*, 3683–3692.

53. Barr, S.D., Ciuffi, A., Leipzig, J., Shinn, P., Ecker, J.R., and Bushman, F.D. (2006). HIV integration site selection: targeting in macrophages and the effects of different routes of viral entry. Mol. Ther. *14*, 218–225.

54. Aiuti, A., Biasco, L., Scaramuzza, S., Ferrua, F., Cicalese, M.P., Baricordi, C., Dionisio, F., Calabria, A., Giannelli, S., Castiello, M.C., et al. (2013). Lentiviral hematopoietic stem cell gene therapy in patients with Wiskott-Aldrich syndrome. Science *80*, 341.

55. Biffi, A., Montini, E., Lorioli, L., Cesani, M., Fumagalli, F., Plati, T., Baldoli, C., Martino, S., Calabria, A., Canale, S., et al. (2013). Lentiviral hematopoietic stem cell gene therapy benefits metachromatic leukodystrophy. Science *80*, 341.

56. Kvaratskhelia, M., Sharma, A., Larue, R.C., Serrao, E., and Engelman, A. (2014). Molecular mechanisms of retroviral integration site selection. Nucleic Acids Res. *42*, 10209–10225.

57. Study to Evaluate the Efficacy and Safety of PF-07055480 / Giroctocogene Fitelparvovec Gene Therapy in Moderately Severe to Severe Hemophilia A Adults (AFFINE) - ClinicalTrials.gov https://clinicaltrials.gov/ct2/show/NCT04370054

58. Gene therapy for haemophilia A - full text view - ClinicalTrials.gov https://clinicaltrials.gov/ct2/show/NCT03001830.

59. A gene transfer study for hemophilia A - full text view - ClinicalTrials.gov https://clinicaltrials.gov/ct2/show/NCT03003533.

60. Shahani, T., Covens, K., Lavend'homme, R., Jazouli, N., Sokal, E., Peerlinck, K., and Jacquemin, M. (2014). Human liver sinusoidal endothelial cells but not hepatocytes contain factor VIII. J. Thromb. Haemost. *12*, 36–42.

61. Everett, L.A., Cleuren, A.C.A., Khoriaty, R.N., and Ginsburg, D. (2014). Murine coagulation factor VIII is synthesized in endothelial cells. Blood *123*, 3697–3705.

62. Fahs, S.A., Hille, M.T., Shi, Q., Weiler, H., and Montgomery, R.R. (2014). A conditional knockout mouse model reveals endothelial cells as the principal and possibly exclusive source of plasma factor VIII. Blood *123*, 3706–3713.

63. Terraube, V., O'Donnell, J.S., and Jenkins, P.V. (2010). Factor VIII and von Willebrand factor interaction: biological, clinical and therapeutic importance. Haemophilia *16*, 3–13.

64. Ozelo, M.C., Vidal, B., Brown, C., Notley, C., Hegadorn, C., Webster, S., Harpell, L., Ahlin, J., Winterborn, A., Handforth, J., et al. (2014). Omental implantation of BOECs in hemophilia dogs results in circulating FVIII antigen and a complex immune response. Blood *123*, 4045–4053.

65. Ormiston, M.L., Toshner, M.R., Kiskin, F.N., Huang, C.J.Z., Groves, E., Morrell, N.W., and Rana, A.A. (2015). Generation and culture of blood outgrowth endothelial cells from human peripheral blood. J. Vis. Exp. *2015*, e53384.

66. Hebbel, R.P. (2017). Blood endothelial cells: utility from ambiguity. J. Clin. Invest. *127*, 1613–1615.

67. Hayakawa, M., Sakata, A., Hayakawa, H., Matsumoto, H., Hiramoto, T., Kashiwakura, Y., Baatartsogt, N., Fukushima, N., Sakata, Y., Suzuki-Inoue, K., et al. (2021). Characterization and visualization of murine coagulation factor VIII-producing cells in vivo. Sci. Rep. *11*, 1–11.

68. Merlin, S., Cannizzo, E.S., Borroni, E., Bruscaggin, V., Schinco, P., Tulalamba, W., Chuah, M.K., Arruda, V.R., VandenDriessche, T., Prat, M., et al. (2017). A novel platform for immune tolerance induction in hemophilia A mice. Mol. Ther. *25*, 1815–1830.

69. Kriz, J., Vilk, G., Mazzuca, D.M., Toleikis, P.M., Foster, P.J., and White, D.J.G. (2012). A novel technique for the transplantation of pancreatic islets within a vascularized device into the greater omentum to achieve insulin independence. Am. J. Surg. *203*, 793–797.

70. A. Safety, tolerability and efficacy study of Sernova's Cell PouchTM for clinical islet transplantation - full text view - ClinicalTrials.Gov https://clinicaltrials.gov/ct2/show/NCT03513939.

71. Hur, J., Yoon, C.H., Kim, H.S., Choi, J.H., Kang, H.J., Hwang, K.K., Oh, B.H., Lee, M.M., and Park, Y.B. (2004). Characterization of two types of endothelial progenitor cells and their different contributions to neovasculogenesis. Arterioscler. Thromb. Vasc. Biol. *24*, 288–293.

72. Zhang, X., Xu, Y., Thomas, V., Bellis, S.L., and Vohra, Y.K. (2011). Engineering an antiplatelet adhesion layer on an electrospun scaffold using porcine endothelial progenitor cells. J. Biomed. Mater. Res. - Part A. *97 A*, 145–151.

73. Bittorf, P., Bergmann, T., Merlin, S., Olgasi, C., Pullig, O., Sanzenbacher, R., Zierau, M., Walles, H., Follenzi, A., and Braspenning, J. (2020). Regulatory-compliant validation of a highly sensitive qPCR for biodistribution assessment of hemophilia A patient cells. Mol. Ther. - Methods Clin. Dev. *18*, 176–188.

74. Kolbe, M., Dohle, E., Katerla, D., Kirkpatrick, C.J., and Fuchs, S. (2010). Enrichment of outgrowth endothelial cells in high and low colony-forming cultures from peripheral blood progenitors. Tissue Eng. - Part C Methods *16*, 877–886.

75. Gillet, N.A., Malani, N., Melamed, A., Gormley, N., Carter, R., Bentley, D., Berry, C., Bushman, F.D., Taylor, G.P., and Bangham, C.R.M. (2011). The host genomic environment of the provirus determines the abundance of HTLV-1-infected T-cell clones. Blood *117*, 3113–3122.

76. Firouzi, S., López, Y., Suzuki, Y., Nakai, K., Sugano, S., Yamochi, T., and Watanabe, T. (2014). Development and validation of a new high-throughput method to investigate the clonality of HTLV-1-infected cells based on provirus integration sites. Genome Med. *6*, 46.

77. Sessa, M., Lorioli, L., Fumagalli, F., Acquati, S., Redaelli, D., Baldoli, C., Canale, S., Lopez, I.D., Morena, F., Calabria, A., et al. (2016). Lentiviral haemopoietic stem-cell gene therapy in early-onset metachromatic leukodystrophy: an ad-hoc analysis of a non-randomised, open-label, phase 1/2 trial. Lancet *388*, 476–487.

78. Spinozzi, G., Calabria, A., Brasca, S., Beretta, S., Merelli, I., Milanesi, L., and Montini, E. (2017). VISPA2: a scalable pipeline for high-throughput identification and annotation of vector integration sites. BMC Bioinform. *18*.

79. Berry, C.C., Gillet, N.A., Melamed, A., Gormley, N., Bangham, C.R.M., and Bushman, F.D. (2012). Estimating abundances of retroviral insertion sites from DNA fragment length data. Bioinformatics *28*, 755–762.

80. Biffi, A., Bartholomae, C.C., Cesana, D., Cartier, N., Aubourg, P., Ranzani, M., Cesani, M., Benedicenti, F., Plati, T., Rubagotti, E., et al. (2011). Lentiviral vector common integration sites in preclinical models and a clinical trial reflect a benign integration bias and not oncogenic selection. Blood *117*, 5332–5339.

81. McLean, C.Y., Bristor, D., Hiller, M., Clarke, S.L., Schaar, B.T., Lowe, C.B., Wenger, A.M., and Bejerano, G. (2010). GREAT improves functional interpretation of *cis*-regulatory regions. Nat. Biotechnol. *28*, 495–501.

82. Liu, Y. (2012). Standardizing a simpler, more sensitive and accurate tail bleeding assay in mice. World J. Exp. Med. *2*, 30.

83. Schuettrumpf, J., Herzog, R.W., Schlachterman, A., Kaufhold, A., Stafford, D.W., and Arruda, V.R. (2005). Factor IX variants improve gene therapy efficacy for hemophilia B. Blood *105*, 2316–2323.

OMTM, Volume *23*

Supplemental information

Efficient and safe correction of hemophilia A by lentiviral vector-transduced BOECs in an implantable device

Cristina Olgasi, Chiara Borsotti, Simone Merlin, Thorsten Bergmann, Patrick Bittorf, Adeolu Badi Adewoye, Nicholas Wragg, Kelcey Patterson, Andrea Calabria, Fabrizio Benedicenti, Alessia Cucci, Alessandra Borchiellini, Berardino Pollio, Eugenio Montini, Delfina M. Mazzuca, Martin Zierau, Alexandra Stolzing, Philip.M. Toleikis, Joris Braspenning, and Antonia Follenzi

Lentiviral vector generation. Third generation self-inactivating LVs were produced as previously published.[1] Briefly, 293T cells were expanded and transiently transfected by the calcium phosphate precipitation method with four plasmids encoding for two core packaging constructs (pMDLg/pol and pRSV-Rev), the envelope construct (pMD.VSV.G), and the transfer vector construct (pVEC.hBDD-FVIII.LV or pVEC.GFP.LV). The cell supernatant was harvested, and LV particles were concentrated by ultracentrifugation. For GMP-grade production of LV, the KR2i TFF System® (Spectrum Lab) was used according to the manufacturer's protocol. The product is ISO 9001:2008 certified. The system consists of a digital peristaltic pump, man/machine interface with a graphical LCD display, digital pressure monitor, KR2i Easy-Load Pump head, Automatic Backpressure Valve, filter module stand, and a real-time data collection software. The Tangential Flow Filtration (TFF) System uses a constant turbulent flow along a porous membrane to eliminate impurities from the sample. The tangential flow along the membrane prevents the accumulation of material on the membrane surface, as opposed to the classical "dead-end filtration", and allows the maximum recovery with high purity of the product.

Analysis of lentiviral vector copy number. Genomic DNA from LV-VEC.hBDD-FVIII and LV-VEC.GFP transduced BOECs was isolated using ReliaPrep gDNA Tissue Miniprep System (Promega). Real-time qPCR was used to evaluate the integrated LV copy numbers per cell in the DNA. Primers used for the qPCR recognize the Wpre sequence: Forward TTGCTTCCCGTATGGCTTTC, Reverse AGCTGACAGGTGGTGGCAAT. Finally, TU/ml was calculated with the following formula: TU/ml = (LV copies/cell × No. of transduced cells) / LV volume (expressed in ml).

Evaluation of HIV-1 p24 in culture medium of transduced BOECs. The presence of HIV-1 p24 was evaluated in culture medium of transduced cells after several time points and passages. Samples were analyzed using Liaison® XL (Diasorin) in the Virology Laboratory of the Hospital (Ospedale Maggiore della Carità di Novara, Italy).

RNA isolation and RT-PCR. Total RNA was isolated by Isol-RNA Lysis Reagent (Invitrogen). One µg of RNA was treated with DNase I (Thermo Scientific), and cDNAs were obtained using the RevertAid First Strand cDNA Synthesis Kit (Thermo Scientific). All PCRs were performed with GoTaq® Flexi DNA Polymerase (Promega). Primers, annealing temperatures, and product sizes are listed below in Supplemental Table 1. PCR products were resolved in 2% agarose gels using 100 bp DNA ladder (Thermo Scientific).

In vitro tubulogenesis assay. Pure Matrigel (BD Bioscience) was added to each well of a 24-well tissue culture plate and allowed to solidify at 37°C for 1 h. A cell suspension containing 10^5 BOECs, resuspended in culture medium, was placed on top of the Matrigel. Plates were incubated at 37°C, 5% CO_2 and observed and imaged at 16 h to detect capillary-like structure formation using an inverted microscope Leica ICC50.

Flow cytometry analysis. BOECs were characterized by flow cytometric analysis using antibodies listed in Supplemental Table 2. For each sample, 1.5×10^5 live events were acquired either on the Attune NxT Acoustic Focusing Cytometer (ThermoFisher Scientific, Waltham, MA, USA) or on BD FACSCanto II. Data were analyzed by FCS Express 6 (DeNovo Software, Glendale, CA, USA) or using FlowJo Software V10.6 (FlowJo LLC).

Histopathological staining and analysis of samples from Cell Pouch™. Sernova Cell Pouches™ with transplanted FVIII-BOECs were explanted from the mice, dissected into segments, fixed in 10% neutral buffered formalin, and paraffin-embedded. Sections (5-6 µM-thick) were stained with hematoxylin and eosin (H&E) and Masson's Trichrome (Nucro-Technics, Scarborough, Ontario).

Immunostaining. For immunofluorescence (IF) staining, BOECs were cultured on plastic and fixed in PFA 4%, for nuclear staining permeabilized in 0,5% PBS-Triton X100 and then incubated with blocking buffer (BB, 5% goat serum, 1% BSA, 0.1% Triton X-100 in PBS) at room temperature (RT). Mouse tissues were fixed in 4% PFA, equilibrated in sucrose, and embedded in cryostat embedding medium (Bio-Optica). Cryostat sections of 4-µm thickness were blocked in BB, incubated with primary antibody at RT, and then incubated in the dark at RT with the secondary antibody. The Cell Pouch™ with transplanted FVIII-BOECs was explanted from each animal, dissected into segments, and immediately cryopreserved in Tissue-Tek® O.C.T. compound (VWR) using an isopentane (2-methylbutane)/dry ice slurry (-70°C), and stored at -80°C. Prior to staining, cryostat sections (5-6 µm) were air-dried and pre-treated by immersion in cold acetone (-20°C), followed by washes in tris-buffered saline (TBS). Sections were blocked in TBS containing 10% goat serum and 1% BSA. A list of the antibodies used in these experiments is provided in Supplemental Table 3.

Histology analysis and preservation techniques of tissues. Following explantation, gross observations of Cell Pouches™ were made and images taken just prior to further histological processing. The 1 Plug Cell Pouches™ were then dissected into 3 segments (a – c) (see Figure 1). Segments 'a' and 'c' were processed for fixation in 10% neutral buffered formalin (Sernova Histology SOP-H900). Cell Pouches™ were washed from 10% formalin in 1X phosphate buffered saline (PBS) to 70% ethanol and subsequently processed for paraffin embedding. Segment 'b' was flash frozen for cryopreservation at the time of dissection using an isopentane/dry ice slurry and embedded in optimal cutting temperature compound (O.C.T.) (Sernova Histology SOP-H936). Cryopreserved or paraffin-embedded segments were then serially sectioned with a cryostat or microtome, respectively.

Preparation of slides and high-resolution images with description of tissue stains. Prior to staining or immunohistochemistry (IHC) analysis, sections were deparaffinized and rehydrated. Sections were stained with H&E for either formalin-fixed paraffin embedded (FFPE) or cryopreserved tissues. Masson's trichrome staining was performed on FFPE (Nucro-Technics, Scarborough, Ontario). For IHC staining, cryopreserved O.C.T. embedded tissues were dried, pre-treated with fixation and permeabilization with cold acetone (-20 ºC, 10 min) and stained to detect microvessel

formation with von Willebrand factor (vWF). For human cell detection, sections were stained with a human leukocyte antigen (HLA-ABC) antibody. High resolution images and full slide scanning of the sections were imaged with an EVOS™ FL Auto 2 Imaging System (Invitrogen™, ThermoFisher Scientific) for both light microscopy (H&E and Masson's Trichrome) and fluorescent IHC (vWF/HLA).

Analysis methodology. The following histological assessment was conducted on the serial sections of formalin-fixed paraffin embedded (FFPE) segments taken within the chambers of each of the Cell Pouches™ from the animals across the doses and explanation time points: 1) stromal development, including type, distribution, and maturity; 2) vascularity, including neovascularization, established vessels, and their respective relationship to the chamber area; 3) inflammation, including type and relative abundance; and 4) hemorrhage. Masson's trichrome stains were assessed for collagen deposition as a marker of stromal maturity. Histological variables were assessed in a semi-quantitative fashion: - absent; + mild; ++ moderate; and +++ marked.

A histological assessment was conducted of the serial sections of frozen embedded segments taken within the chambers of each of the Cell Pouches™ from the animals across the doses and explanation time points: 1) cell transplant survival; 2) interactions and development post-transplant; 3) interactions of the surrounding pre-vascularized tissue of the Cell Pouch™; and 4) blood vessel formation relative to transplant cells. Histological variables were assessed in a semi-quantitative fashion: - negative (no staining); +/- equivocal staining; + mild positivity; ++ moderate positivity; +++ marked positivity; n/a image not available.

For histological assessment the slides and high-resolution images were sent to a certified pathologist for analysis. The assessment was conducted in a blinded-fashion, with no knowledge of the animal time points. The assessment was unblinded for writing the final report. Pathological definitions were as follows: Fibroblastic stroma – mesenchymal tissue consisting of fibroblastic cells and the extracellular matrix, including variable collagen produced by these cells; Collagen – usually a fibrillar protein within the extracellular matrix of connective tissue that provides mechanical strength to the tissues; Neovascularization – tiny, immature capillary-like vessels arising during new blood vessel formation and growth.

A

Name of donor	Donor	Mutation	ml of peripheral blood samples	No. of BOECs colonies
pHA1	Severe HA	c.6273G>A exon 21	25	30
pA	Severe HA	intron 22 inversion	22	60
pC	Severe HA	unknown	25	40
pD	Severe HA	intron 22 inversion	26	30

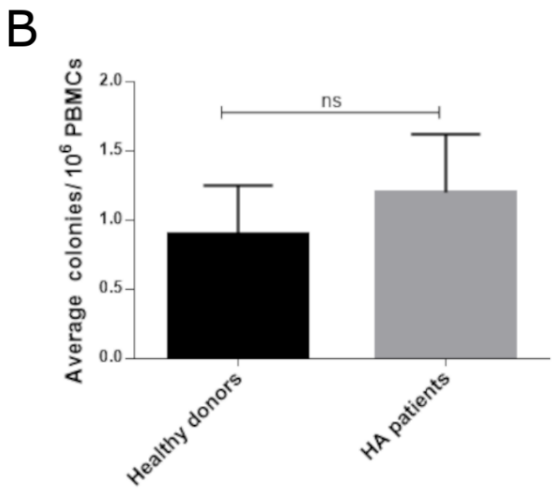

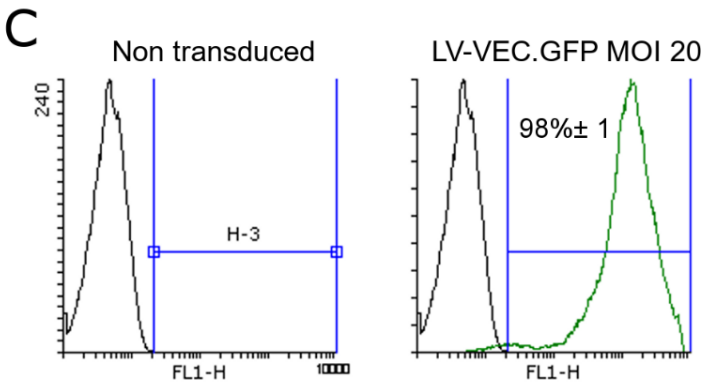

Figure S 1. (A) List of hemophilic patients from whom BOECs were isolated. (B) Average number of colonies calculated on 10^6 PBMCs cultured. Statistical analysis was performed using t-test, non-parametric, p-value 0.098. (C) Representative histograms for GFP evaluation by FACS analysis in healthy and HA BOECs transduced with an MOI of 20.

A

Sample	LV copy number/ cell
Healthy BOECs	0
LV-VEC.GFP Healthy BOECs	5.2± 0.6
LV-VEC.hBDD-FVIII Healthy BOECs	3.1± 0.5
HA BOECs	0
LV-VEC.GFP HA BOECs	6.2± 0.8
LV-VEC.hBDD-FVIII HA BOECs	3±0.2

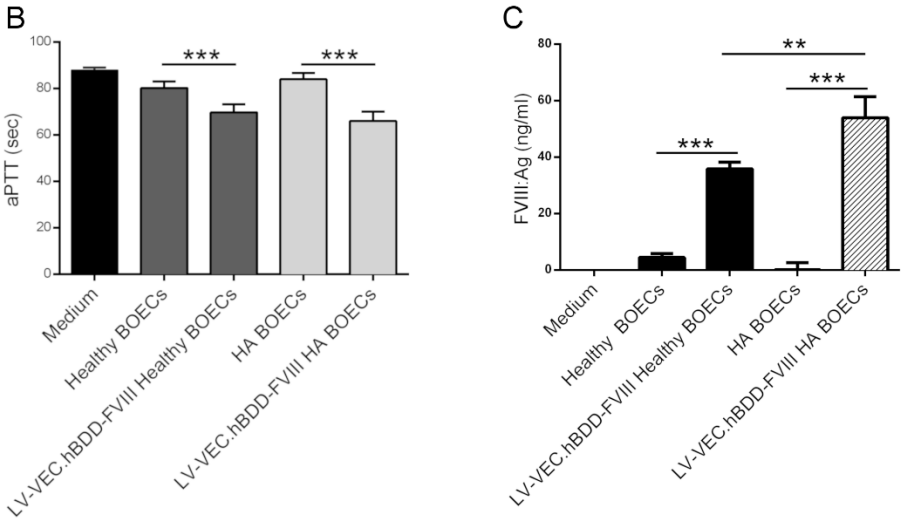

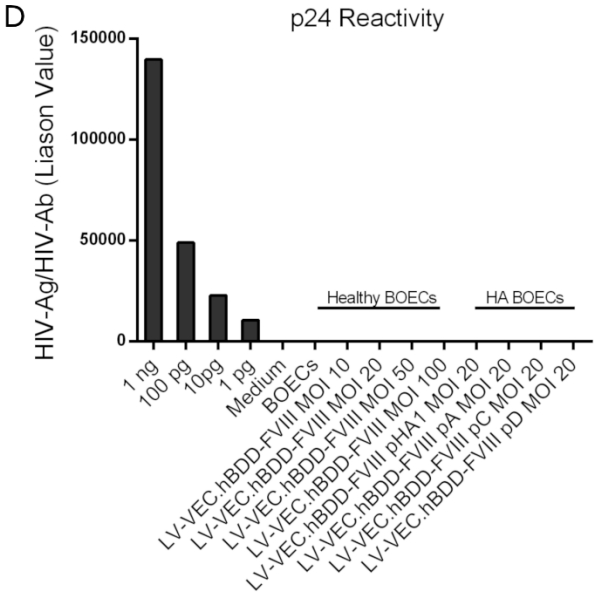

Figure S2. (A) qPCR analysis of integrated LV copy number/cell. (**B**) aPTT assay on supernatant of transduced and non-transduced healthy and HA BOECs (**C**) Antigen assay on supernatant of transduced and non-transduced healthy and HA BOECs. Data are expressed as mean ± SD and are representative of four independent experiments. (**D**) HIV-1 p24 analysis on medium of non-transduced and transduced and healthy and HA BOECs at different MOIs.

Table S1. Histological features of NSG-HA Cell Pouches™ transplanted with FVIII-BOECs (H&E and Trichrome).

Animal ID	Inflammation	Fibroblastic stroma	Collagen deposition	Neovascularization	Established vessels	Hemorrhage
Cell Lot HA1, 4 weeks, 10×10^6 (Dose 1)						
396-LEP	-	+++	+	++	*	-
398-REP	-	+++	++	++	++	-
Cell Lot HA1, 4 weeks, 5×10^6 (Dose 2)						
397-LEP	-	+	+	+	*	-
397-BEP	-	+++	+++	++	++	-
Cell Lot HA1, 4 weeks, 2×10^6 (Dose 3)						
398-BEP	-	+++	+	++	*	-
Cell Lot HA1, 8 weeks, 10×10^6 (Dose 1)						
405-NEP	-	+++	+++	++	++	-
Cell Lot HA1, 8 weeks, 5×10^6 (Dose 2)						
414-NEP	-	+++	+	++	+	-
415-BEP	-	+++	+++	++	+	-
Cell Lot HA1, 8 weeks, 2×10^6 (Dose 3)						
402-LEP	-	+++	++	++	++	-
405-REP	-	++	+	++	+	-
413-LEP	-	++	+++	++	*	-
Cell Lot HA1, 12 weeks, 10×10^6 (Dose 1)						
399-NEP	-	+++	++	++	+	-
413-BEP	-	+++	+++	++	++	-
Cell Lot HA1, 12 weeks, 5×10^6 (Dose 2)						
406-REP	-	+++	++	++	*	-
406-NEP	-	+++	++	++	+	-
411-BEP	-	+++	+++	+	++	-
Cell Lot HA1, 12 weeks, 2×10^6 (Dose 3)						
396-REP	-	+++	+++	+	+	+
398-NEP	-	+++	++	++	+	-
399-BEP	-	+++	++	++	+	-
Cell Lot HAA, 4 weeks, 10×10^6 (Dose 1)						
520-RREP	-	+++	++	++	++	-
Cell Lot HAA, 4 weeks, 5×10^6 (Dose 2)						
523-LEP	-	+++	++	++	+	-
Cell Lot HAA, 8 weeks, 10×10^6 (Dose 1)						
520-NEP	-	+++	+++	++	+	-
524-LEP	-	+++	+++	++	++	-
Cell Lot HAA, 8 weeks, 5×10^6 (Dose 2)						
523-REP	-	+++	++	++	++	-
Cell Lot HAA, 12 weeks, 10×10^6 (Dose 1)						
522-RREP	-	+++	++	++	++	-
524-BEP	-	+++	++	++	++	-
Controls (no cell transplant)						
4 weeks						
525-REP	-	++	++	++	+	-
8 weeks						
521-RREP	-	+++	++	++	++	-
525-RREP	-	+++	+	++	++	-
12 weeks						
403-NEP	-	+++	+	++	+	-
521-BEP	-	+++	++	++	++	-
525-BEP	-	+++	++	++	++	-

*present immediately adjacent to Cell Pouch™

Table S2. Immunofluorescence of NSG-HA Mouse Cell Pouches™ transplanted with FVIII-BOECs.

Animal ID	HLA-ABC (red)	vWF (green)
Cell Lot HA1, 4 weeks, 10×10^6 (Dose 1)		
396-LEP	+	+
398-REP	+	+
Cell Lot HA1, 4 weeks, 5×10^6 (Dose 2)		
397-REP	+	+
397-LEP	n/a	n/a
414-LEP	+/-	+
Cell Lot HA1, 4 weeks, 2×10^6 (Dose 3)		
398-BEP	-	++
Cell Lot HA1, 8 weeks, 10×10^6 (Dose 1)		
405-NEP	++	-
Cell Lot HA1, 8 weeks, 5×10^6 (Dose 2)		
414-NEP	+	n/a
415-BEP	+/-	+
Cell Lot HA1, 8 weeks, 2×10^6 (Dose 3)		
402-LEP	+/-	+
405-REP	+/-	+
413-LEP	n/a	n/a
Cell Lot HA1, 12 weeks, 10×10^6 (Dose 1)		
399-NEP	-	n/a
413-BEP	+/-	+
Cell Lot HA1, 12 weeks, 5×10^6 (Dose 2)		
406-REP	+	+
406-NEP	+/-	++
411-BEP	+/-	+
Cell Lot HA1, 12 weeks, 2×10^6 (Dose 3)		
396-REP	+/-	+
398-NEP	+	+
399-BEP	+/-	+
Cell Lot HAA, 4 weeks, 10×10^6 (Dose 1)		
520-RREP	++	++
Cell Lot HAA, 4 weeks, 5×10^6 (Dose 2)		
520-REP	++	+
523-LEP	+++	+++
Cell Lot HAA, 8 weeks, 10×10^6 (Dose 1)		
520-NEP	++	+
524-LEP	+	+
Cell Lot HAA, 8 weeks, 5×10^6 (Dose 2)		
523-REP	-	+++
Cell Lot HAA, 12 weeks, 10×10^6 (Dose 1)		
522-RREP	++	++
524-BEP	+++	+
Controls		
4 weeks		
525-REP	-	++
8 weeks		
521-RREP	-	N/A
525-RREP	-	+
12 weeks		
403-NEP	-	+
521-BEP	-	+
525-BEP	-	+

- negative (no staining); +/- equivocal staining; + mild positivity; ++ moderate positivity; +++ marked positivity; N/A image not available

Table S3. Summary of sequencing reads and IS retrieved by group. Non redundant IS (column N.IS) retrieved from Healthy or HA Donors and transduced with VEC-FVIII or VEC-GFP were grouped. IS shared between different time points of the same transduction are counted once.

Group	Donor	Transduction	Vector	MOI	Timepoint	Sample ID	N.IS
Healthy.GFP	D45	4	VEC-GFP	10+10	P5	BOEC-008	1,862
Healthy.FVIII	D45	1	VEC-FVIII	20	P5	BOEC-001	5,864
					P8	BOEC-002	
					P11	BOEC-003	
					P15	BOEC-004	
					70 days HA Beads	BOEC-010	
					70 days HA Beads	BOEC-011	
					70 days HA Beads	BOEC-013	
		2	VEC-FVIII	30	P11	BOEC-005	
		3		50	P11	BOEC-006	
	D2	5	VEC-FVIII	20	P5	BOEC-014	
					P8	BOEC-043A	
	D3	6	VEC-FVIII	20	P5	BOEC-043B	
					P8	BOEC-043C	
HA.GFP	pHA1	8	VEC-GFP	20	P5	BOEC-020	106,554
					P8	BOEC-021	
					P12	BOEC-022	
	pA	10	VEC-GFP	20	P5	BOEC-032	
					P8	BOEC-033	
	pC	12	VEC-GFP	20	P5	BOEC-040	
					P8	BOEC-041	
HA.FVIII	pHA1	7	VEC-FVIII	20	P5	BOEC-016	28,069
					P8	BOEC-017	
					P10	BOEC-018	
					P15	BOEC-019	
					P11	BOEC-024	
					P11	BOEC-025	
					P14	BOEC-026	
					P11	HA1-VEC-UNILO	
					91 days HA Beads	BOEC-044A	
					91 days HA Beads	BOEC-044B	
					91 days HA Beads	BOEC-044C	
					2 weeks Cell Pouch	397-LEP	
					2 weeks Cell Pouch	398-LEP	
					4 weeks Cell Pouch	398-BEP	
					4 weeks Cell Pouch	414-LEP	
					4 weeks Cell Pouch	396-LEP	
					8 weeks Cell Pouch	402-LEP	
					8 weeks Cell Pouch	415-BEP	
					8 weeks Cell Pouch	405-NEP	
					12 weeks Cell Pouch	398-NEP	
					12 weeks Cell Pouch	406-REP	
					12 weeks Cell Pouch	399-NEP	
	pA	9	VEC-FVIII	20	P5	BOEC-027	
					P8	BOEC-028	
					P10	BOEC-029	
					P14	HA-A-p14	
					P15	BOEC-030	
					P12	BOEC-031	
					112 days HA Beads	BOEC-045A	
					112 days HA Beads	BOEC-045B	
					112 days HA Beads	BOEC-045C	
					4 weeks Cell Pouch	520-REP	
					4 weeks Cell Pouch	520-RREP	
					8 weeks Cell Pouch	520-LEP	
					8 weeks Cell Pouch	520-NEP	
					12 weeks Cell Pouch	522-RREP	
	pC	11	VEC-FVIII	20	P5	BOEC-035	
					P8	BOEC-036	
					P8	HA-C-p8	
					P10	BOEC-037	
					P11	BOEC-039	
					P14	HA-C-p14	
					P15	BOEC-038	
					P19	HA-C-p19	
					112 days HA Beads	BOEC-046A	
					112 days HA Beads	BOEC-046B	
					112 days HA Beads	BOEC-046C	
	pD	13	VEC-FVIII	20	P16	HA-D-p16	
	TOTAL						142,349

Table S4. Gene Ontology (GO) enrichment for Molecular Function and Biological Process. IS coordinates from IS retrieved from HA.VEC-FVIII, HA.VEC-GFP, Healthy.VEC-FVIII, and Healthy.VEC-GFP were analyzed by G.R.E.A.T. enrichment discovery algorithms. GO Biological Process, Molecular Function and Cellular Component databases highlighted significantly overrepresented gene classes. The gene classes found in at least two groups are highlighted in pink.

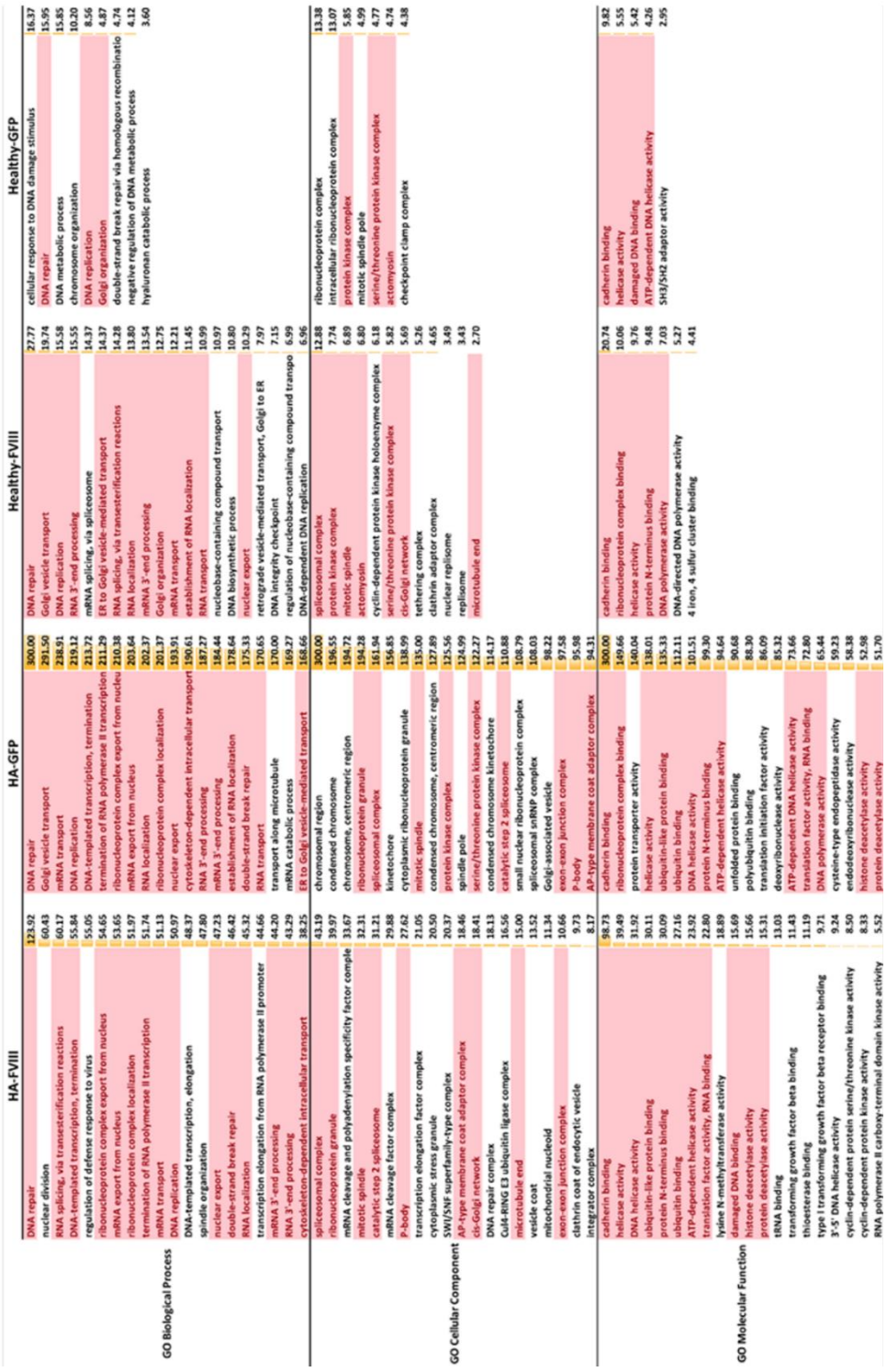

	HA-FVIII		HA-GFP		Healthy-FVIII		Healthy-GFP	
GO Biological Process	DNA repair	123.92	DNA repair	300.00	DNA repair	27.77	cellular response to DNA damage stimulus	16.37
	nuclear division	60.43	Golgi vesicle transport	291.50	Golgi vesicle transport	19.74	DNA repair	15.95
	RNA splicing, via transesterification reactions	60.17	mRNA transport	238.91	DNA replication	15.58	DNA metabolic process	15.85
	DNA-templated transcription, termination	55.84	DNA replication	219.12	RNA 3'-end processing	15.55	chromosome organization	10.20
	regulation of defense response to virus	55.05	DNA-templated transcription, termination	213.72	mRNA splicing, via spliceosome	14.37	DNA replication	8.56
	ribonucleoprotein complex export from nucleus	54.65	termination of RNA polymerase II transcription	211.29	ER to Golgi vesicle-mediated transport	14.37	Golgi organization	4.87
	mRNA export from nucleus	53.65	ribonucleoprotein complex export from nucleu	210.38	RNA splicing, via transesterification reactions	14.28	double-strand break repair via homologous recombinatio	4.74
	ribonucleoprotein complex localization	51.97	mRNA export from nucleus	203.64	RNA localization	13.80	negative regulation of DNA metabolic process	4.12
	termination of RNA polymerase II transcription	51.74	RNA localization	202.37	mRNA 3'-end processing	13.54	hyaluronan catabolic process	3.60
	mRNA transport	51.13	ribonucleoprotein complex localization	201.37	Golgi organization	12.75		
	DNA replication	50.97	nuclear export	193.91	mRNA transport	12.21		
	DNA-templated transcription, elongation	48.37	cytoskeleton-dependent intracellular transport	190.61	establishment of RNA localization	11.45		
	spindle organization	47.80	RNA 3'-end processing	187.27	RNA transport	10.99		
	nuclear export	47.23	mRNA 3'-end processing	184.44	nucleobase-containing compound transport	10.97		
	double-strand break repair	46.42	establishment of RNA localization	178.64	DNA biosynthetic process	10.80		
	RNA localization	45.32	double-strand break repair	175.33	nuclear export	10.29		
	transcription elongation from RNA polymerase II promoter	44.66	RNA transport	170.65	retrograde vesicle-mediated transport, Golgi to ER	7.97		
	mRNA 3'-end processing	44.20	transport along microtubule	170.00	DNA integrity checkpoint	7.15		
	RNA 3'-end processing	43.29	mRNA catabolic process	169.27	regulation of nucleobase-containing compound transpo	6.99		
	cytoskeleton-dependent intracellular transport	38.25	ER to Golgi vesicle-mediated transport	168.66	DNA-dependent DNA replication	6.96		
GO Cellular Component	spliceosomal complex	43.19	chromosomal region	300.00	spliceosomal complex	12.88	ribonucleoprotein complex	13.38
	ribonucleoprotein granule	39.97	condensed chromosome	196.55	protein kinase complex	7.74	intracellular ribonucleoprotein complex	13.07
	mRNA cleavage and polyadenylation specificity factor comple	33.67	chromosome, centromeric region	194.72	mitotic spindle	6.89	protein kinase complex	5.85
	mitotic spindle	32.31	ribonucleoprotein granule	194.28	actomyosin	6.80	mitotic spindle pole	4.99
	catalytic step 2 spliceosome	31.21	spliceosomal complex	161.94	cyclin-dependent protein kinase holoenzyme complex	6.18	serine/threonine protein kinase complex	4.77
	mRNA cleavage factor complex	29.88	kinetochore	156.85	serine/threonine protein kinase complex	5.82	actomyosin	4.74
	P-body	27.62	cytoplasmic ribonucleoprotein granule	138.99	cis-Golgi network	5.69	checkpoint clamp complex	4.38
	transcription elongation factor complex	21.05	mitotic spindle	135.00	tethering complex	5.26		
	cytoplasmic stress granule	20.50	condensed chromosome, centromeric region	127.89	clathrin adaptor complex	4.65		
	SWI/SNF superfamily-type complex	20.37	protein kinase complex	125.56	nuclear replisome	3.49		
	AP-type membrane coat adaptor complex	18.46	spindle pole	124.99	replisome	3.43		
	cis-Golgi network	18.41	serine/threonine protein kinase complex	122.27	microtubule end	2.70		
	DNA repair complex	18.13	condensed chromosome kinetochore	114.17				
	Cul4-RING E3 ubiquitin ligase complex	16.56	catalytic step 2 spliceosome	110.88				
	microtubule end	15.00	small nuclear ribonucleoprotein complex	108.79				
	vesicle coat	13.52	spliceosomal snRNP complex	108.03				
	mitochondrial nucleoid	11.34	Golgi-associated vesicle	58.22				
	exon-exon junction complex	10.66	exon-exon junction complex	97.58				
	clathrin coat of endocytic vesicle	9.73	P-body	95.98				
	integrator complex	8.17	AP-type membrane coat adaptor complex	94.31				
GO Molecular Function	cadherin binding	58.73	cadherin binding	300.00	cadherin binding	20.74	cadherin binding	9.82
	helicase activity	39.49	ribonucleoprotein complex binding	169.66	ribonucleoprotein complex binding	10.06	helicase activity	5.55
	DNA helicase activity	31.92	protein transporter activity	140.04	helicase activity	9.76	damaged DNA binding	5.42
	ubiquitin-like protein binding	30.11	helicase activity	138.01	protein N-terminus binding	9.48	ATP-dependent DNA helicase activity	4.26
	protein N-terminus binding	30.09	ubiquitin-like protein binding	135.33	DNA polymerase activity	7.03	SH3/SH2 adaptor activity	2.95
	ubiquitin binding	27.16	ubiquitin binding	112.11	DNA-directed DNA polymerase activity	5.27		
	ATP-dependent helicase activity	23.92	DNA helicase activity	101.51	4 iron, 4 sulfur cluster binding	4.41		
	translation factor activity, RNA binding	22.80	protein N-terminus binding	99.30				
	lysine N-methyltransferase activity	18.89	ATP-dependent helicase activity	94.64				
	damaged DNA binding	15.69	unfolded protein binding	90.68				
	histone deacetylase activity	15.66	polyubiquitin binding	88.30				
	protein deacetylase activity	15.31	translation initiation factor activity	86.09				
	tRNA binding	13.03	deoxyribonuclease activity	85.32				
	transforming growth factor beta binding	11.43	ATP-dependent DNA helicase activity	73.66				
	thioesterase binding	11.19	translation factor activity, RNA binding	72.80				
	type I transforming growth factor beta receptor binding	9.71	DNA polymerase activity	65.44				
	3'-5' DNA helicase activity	9.24	cysteine-type endopeptidase activity	59.23				
	cyclin-dependent protein serine/threonine kinase activity	8.50	endodeoxyribonuclease activity	58.38				
	cyclin-dependent protein kinase activity	8.33	histone deacetylase activity	52.98				
	RNA polymerase II carboxy-terminal domain kinase activity	5.52	protein deacetylase activity	51.70				

Table S5. Common Insertion site (CIS) analysis in 2 healthy BOECs, and 4 HA BOECs.

Subject ID	Transduction	Vector	MOI	Gene Name	Chr.	Integration locus	N IS per Gene	average transcript length	integration frequency with tolerance	tdist fdr
dD3	6	VEC-FVIII	20	SPG7	16	89,585,048	5	39,358	0.036	0.078
dD45	1	VEC-FVIII	20	SZT2	1	43,952,080	13	64,363	0.079	0.006
				MROH1	8	145,269,797	10	89,530	0.053	0.054
				TRAF2	9	139,825,912	6	40,103	0.043	0.114
				CPSF1	8	145,629,805	5	16,288	0.043	0.114
dD45	4	VEC-GFP	10+10	NPLOC4	17	79,591,992	10	36,856	0.073	0.005
				TRAF2	9	139,825,791	8	40,103	0.057	0.020
pA	10	VEC-GFP	20	SZT2	1	43,955,802	117	64,363	0.712	0.510
				NPLOC4	17	79,602,479	106	36,856	0.775	0.510
pA	9	VEC-FVIII	20	NPLOC4	17	79,600,522	7	36,856	0.051	0.067
				PMPCA	9	139,315,510	5	13,189	0.044	0.108
pC	11	VEC-FVIII	20	SZT2	1	43,955,797	49	64,363	0.298	0.039
				MROH1	8	145,299,016	46	89,530	0.243	0.097
				NPLOC4	17	79,600,496	45	36,856	0.329	0.032
pD	13	VEC-FVIII	20	NSD1	5	176,707,259	10	166,759	0.037	0.100
				ZGPAT	20	62,354,996	6	28,232	0.047	0.047
				NONO	X	70,517,315	5	17,977	0.042	0.074
				MAN1B1	9	139,997,714	4	22,261	0.033	0.139
				PTBP1	19	808,672	4	14,936	0.035	0.122
pHA1	7	VEC-FVIII	20	PHRF1	11	599,765	8	35,777	0.059	0.077
				ZNF251	8	145,983,504	8	34,677	0.059	0.077
pHA1	8	VEC-GFP	20	MROH1	8	145,292,887	121	89,530	0.638	0.337
				SZT2	1	43,954,990	112	64,363	0.681	0.337
				NPLOC4	17	79,599,815	94	36,856	0.687	0.337
				ZNF251	8	145,987,938	77	34,677	0.572	0.361

Table S6. Primers used in RT-PCR and Real Time.

Gene	Synthetic oligonucleotide	Expected band
ACTB	F: 5'-GAGAAAATCTGGCACCACACC-3'	412 bp
	R: 5'-CGACGTAGCACAGCTTCTC-3'	
KDR	F: 5'- TGCAAGGACCAAGGAGACTATGT -3'	459 bp
	R: 5'- TAGGATGATGACAAGAAGTAGCC -3'	
TEK	F: 5'-AGACCAGCACGTTGATGTGA-3'	127 bp
	R: 5'-TGGGTTGCTTGACCCTATGT-3'	
CDH5	F: 5'-CAGCCCAAAGTGTGTGAGAA-3'	162 bp
	R: 5'-TGTGATGTTGGCCGTGTTAT-3'	
PECAM1	F: 5'-AGGTCAGCAGCATCGTGGTCAACAT-3'	469 bp
	R: 5'-GTGGGGTTGTCTTTGAATACCGCAG-3'	
VWF	F: 5'- TGGAGTACCCCTTCAGCGAG -3'	263 bp
	R: 5'- GTTGGCATTAGGGCCCACTC -3'	
F8 A2-A3 domain	F: 5'- TGCCACAACTCAGACTTTCG-3'	184 bp
	R: 5'- GATGGCGTTTCAAGACTGGT -3'	
IFI27	F: 5'- TCTGGCTCTGCCGTAGTTTT-3'	243 bp
	R: 5'- GAACTTGGTCAATCCGGAGA -3'	
CDH11	F: 5'- TGGCAGCAAGTATCCAATGG-3'	200 bp
	R: 5'- TTTGGTTACGTGGTAGGCAC-3'	
NRCAM	F: 5'- TCCAGAAGGCAATGCAAGTA-3'	117 bp
	R: 5'- AGCATTCCATCTTCCTTTGC -3'	
COL4A1	F: 5'- GGCCTATGAGTCCTGGGTAC -3'	146 bp
	R: 5'- TGGATTTCAGGGGATGCCAG -3'	
ENG	F: 5'- CCACTGCACTTGGCCTACA -3'	107 bp
	R: 5'- GCCCACTCAAGGATCTGG -3'	
GATA3	F: 5'- GAACCGGCCCCTCATTAAG-3'	216 bp
	R: 5'- CTTGCATATCTGACCTATTCTAGCGTG-3'	
ITGA5	F: 5'- TGCAGTGTGAGGCTGTGTACA -3'	88 bp
	R: 5'- GTGGCCACCTGACGCTCT -3'	
ETS-1	F: 5'- CATATCAAGTTAATGGAGTC-3'	268 bp
	R: 5'- TGTTTGATAGCAAAGTAGTC -3'	
ETS-2	F: 5'- GTGGAGTGAGCAACAGGTAT-3'	282 bp
	R: 5'- CCAAAACCTAATGTATTGCTG -3'	
Wpre/ dNEF	F: 5'- TCTGGCTCTGCCGTAGTTTT-3'	200 bp
	R: 5'- GGCTAAGATCTACAGCTGCCTTG-3'	

Table S7. Antibodies used for FACS staining.

Antibody	Reactivity	Manufacturer	Format
CD45	Human	clone 32D12, Miltenyi Biotec	PE
Isotype mouse IgG1		ThermoFisher Scientific	PE
CD34	Human	clone 4H11[APG], Invitrogen	PE
Isotype mouse IgG1		ThermoFisher Scientific	PE
Anti -mouse	Mouse	Thermo Scientific	488
FVIII	Human	Clone GMA-8015, Green Mountain	Not conjugated

KDR	Human	clone ES8-20E6, Miltenyi Biotec	PE
Isotype mouse IgG1		ThermoFisher Scientific	PE
Tie-2	Human	clone REA198, Miltenyi Biotec	PE
REA Control Antibody, human IgG1, REAfinity (REA293)		Miltenyi Biotec	PE
CD31	Human	clone MEM-05; Invitrogen	APC
Isotype mouse IgG1		ThermoFisher Scientific	APC
VE-cadherin	Human	clone REA199, Miltenyi Biotec	PE
REA Control Antibody, human IgG1, REAfinity (REA293)		Miltenyi Biotec	PE

Table S8. Antibodies used for immunofluorescence staining.

Primary antibodies	**Host**	**Reactivity**	**Manufacturer**	**Dilution**
FVIII	Mouse	Human	Clone GMA-8015, Green Mountain	1:100
CD31	Mouse	Human	BD Bioscience	1:100
HLA-ABC	Rat	Human	Novus Biologicals, clone YTH862.2	1:150
von Willebrand Factor	Rabbit	H, M, R	Millipore	1:100
GFP	Rabbit		Life Technologies	1:300
Secondary antibodies	**Fluorophores**		**Manufacturer**	**Dilution**
Goat anti-Rabbit	AlexaFluor 488 or 546		Life Technologies	1:500/1:1000
Goat anti-Rat	AlexaFluor 594			1:500
Goat anti-Mouse	AlexaFluor 488 or 546		Life Technologies	1:500

Supplemental References

1. Follenzi, A., and Naldini, L. (2002). Generation of HIV- 1 derived lentiviral vectors. Methods Enzymol *346*, 454–465.